Quarter-Scale Close-in Blast-Loading Experiments in Support of the Planned Contained Firing Facility

John W. Pastrnak
Charles E Baker
Larry F. Simmons

The University of California
Lawrence Livermore National Laboratory
P.O. Box 808
Livermore, CA 94551, USA

Abstract

In anticipation of increasingly stringent environmental regulations, Lawrence Livermore National Laboratory is proposing to construct a 60-kg firing chamber to provide blast-effects containment for most of its open-air, high-explosive, firing operations. Even though the Laboratory's operations are within current environmental limits, containment of the blast effects and hazardous debris will drastically reduce emissions to the environment and minimize the generated hazardous waste.

One of the main design considerations is the extremely close-in ($Z = 0.66$ ft/lb$^{1/3}$) blast loading on the reinforced concrete floor of the chamber. Historically, floor damage due to close-in loading has been a common problem for other blast chambers within the U.S. Department of Energy and Department of Defense (DOE/DoD).

Blast-effects testing and computer analysis were conducted on a replica quarter-scale model of the preliminary floor design. Nineteen blast tests ranging from scaled distances of 1.14 ft/1b$^{1/3}$ (25%) to 0.57 ft/lb$^{1/3}$ (200%) were performed on the strain-gaged floor model. In response to predicted and measured failures at the 25% level, various state-of-the-art blast attenuation systems were quickly developed and tested. The most effective blast-attenuation system provided a significant improvement by reducing the measured floor stresses to acceptable levels while minimizing, by its reusability, the impact on the environment.

Background

Lawrence Livermore National Laboratory (LLNL) has conducted open-air explosives detonations at its Site 300 remote test complex since its inception in 1955. The Laboratory uses its explosives test facilities to precisely measure critical variables that are important to nuclear weapon designs, to test conventional ordnance design, and to evaluate possible accidents (such as fires) involving explosives. Open-air testing at LLNL's facilities results in emissions to the environment that comply with all current environmental standards. However, in anticipation of stricter environmental regulations and because of the Secretary of Energy's

Report Documentation Page

Form Approved
OMB No. 0704-0188

1. REPORT DATE	2. REPORT TYPE	3. DATES COVERED
AUG 1994		**00-00-1994 to 00-00-1994**

4. TITLE AND SUBTITLE	5a. CONTRACT NUMBER
Quarter-Scale Close-in Blast-Loading Experiments in Support of the Planned Contained Firing Facility	5b. GRANT NUMBER
	5c. PROGRAM ELEMENT NUMBER
6. AUTHOR(S)	5d. PROJECT NUMBER
	5e. TASK NUMBER
	5f. WORK UNIT NUMBER
7. PERFORMING ORGANIZATION NAME(S) AND ADDRESS(ES) **The University of California,Lawrence Livermore National Laboratory,P.O. Box 808,Livermore,CA,94551**	8. PERFORMING ORGANIZATION REPORT NUMBER
9. SPONSORING/MONITORING AGENCY NAME(S) AND ADDRESS(ES)	10. SPONSOR/MONITOR'S ACRONYM(S)
	11. SPONSOR/MONITOR'S REPORT NUMBER(S)

12. DISTRIBUTION/AVAILABILITY STATEMENT
Approved for public release; distribution unlimited

13. SUPPLEMENTARY NOTES
See also ADM000767. Proceedings of the Twenty-Sixth DoD Explosives Safety Seminar Held in Miami, FL on 16-18 August 1994.

14. ABSTRACT
see report

15. SUBJECT TERMS

16. SECURITY CLASSIFICATION OF:			17. LIMITATION OF ABSTRACT	18. NUMBER OF PAGES	19a. NAME OF RESPONSIBLE PERSON
a. REPORT **unclassified**	b. ABSTRACT **unclassified**	c. THIS PAGE **unclassified**	**Same as Report (SAR)**	**37**	

mandate that environment, safety, and health (ES&H) concerns be the first priority at all DOE facilities, LLNL is developing a comprehensive state-of-the-art blast-effects containment (or contained-firing) facility to reduce emissions of hazardous materials and the amount of contaminated wastes generated by explosives testing. The rationale for the contained-firing concept is to minimize emissions to the environment and reduce quantities of hazardous waste while providing a continuing capability to test nuclear and other assemblies that contain high explosives.

A conceptual design report (CDR)[1,2] for the Contained Firing Facility (CFF) was recently completed whereby a permanent state-of-the-art firing chamber is to be constructed around an existing facility's open-air firing surface to completely contain blast effects and thereby provide enhanced environmental protection, waste minimization, and safety for the 21st century.

Description

Figure 1 is an artist's concept of the CFF to be built around Bunker 801 at LLNL's Site 300 experimental test site. Bunker 801 was chosen because it is the site of LLNL's existing world-class 17-MeV Flash X-Ray (FXR) facility. Bunker 801 already contains a great variety of high-speed optical and electronic diagnostic equipment, which, together with the FXR, provide unique diagnostic capability.

Figure 1. Artist's concept of the planned Contained Firing Facility.

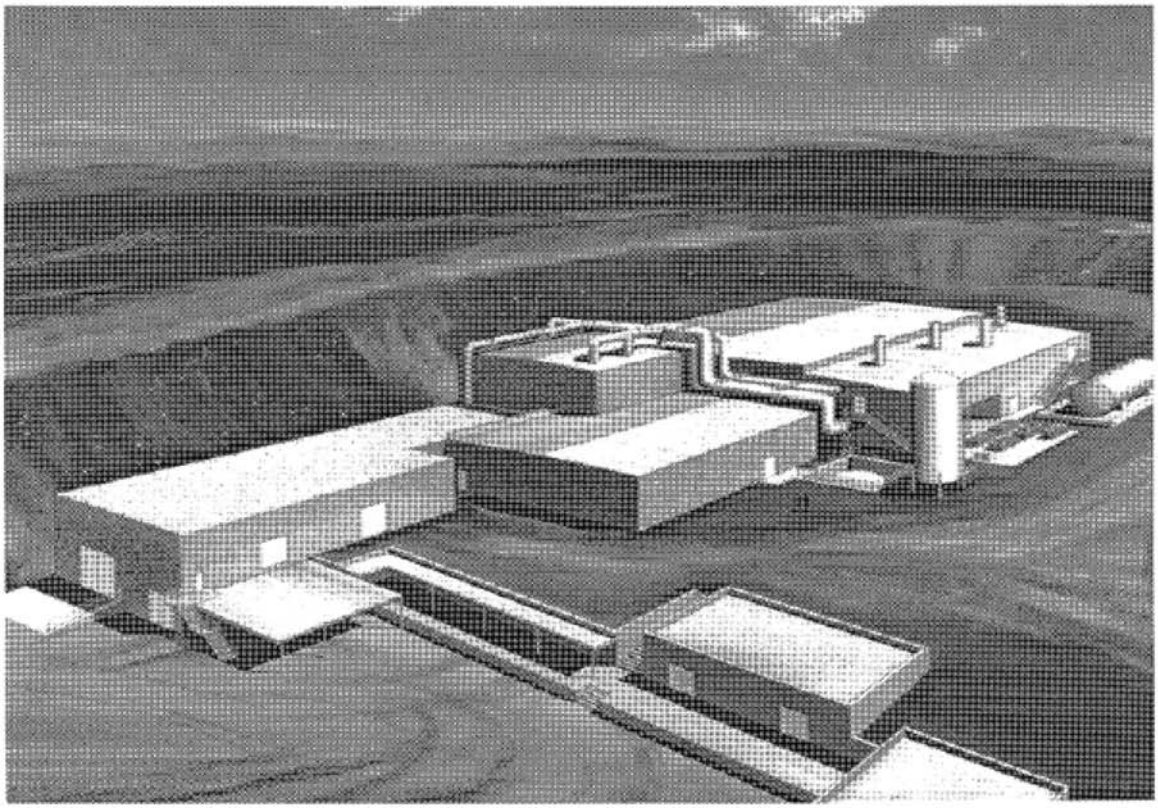

Figure 1. Artist's concept of the planned Contained Firing Facility.

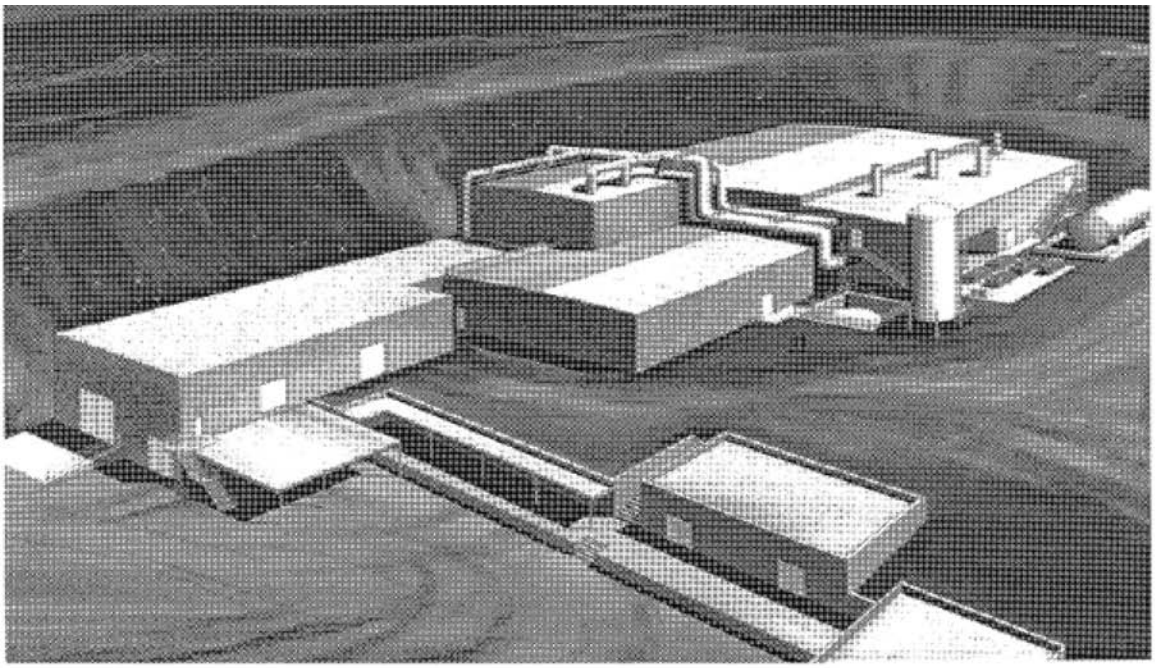

Figure 1. Artist's concept of the planned Contained Firing Facility.

The heart of the CFF is the firing chamber, slightly larger than half a gymnasium, which will contain the blast overpressure and fragmentation effects from detonations of cased explosive charges up to 60 kg. The inside surfaces of the chamber are to be protected from high-velocity shrapnel fragments that result from detonations of cased explosives. To permit repetitive firings, all main structural elements of the firing chamber are to be designed to remain elastic when subjected to blast. The detonations are to be conducted above a 150-mm-thick steel firing surface (the shot anvil) embedded in the floor. The CFF project consists of adding approximately 2463 m^2 of structural additions to the existing open-air firing facility at Bunker 801. The structural additions consist of four components: the firing chamber, a support facility, a diagnostic equipment facility, and an office/conference module, as shown in Fig. 2.

Explosive quantity zones, which vary in operational mass up to 60 kg of PBX-9404 (a plastic bonded explosive containing 94% HMX)[3] or an equivalent TNT weight of 206 lb are shown in Fig. 3 for detonations at the nominal distance of 1.22 m above the anvil surface. Separate, general-purpose, removable shielding protects the interior surfaces of the firing chamber from high-velocity fragments. A key aspect of the CFF is that the firing chamber is rectangular and is designed to use low-cost conventional reinforced concrete, as opposed to labor-intensive lacing reinforcement commonly found in most blast-resistant structural designs. From a materials standpoint, a spherical chamber shape would be more efficient, but a rectangular shape is cheaper to fabricate overall, provides easier and more desirable setup and working surfaces, and encompasses existing diagnostic systems. The thickness of the reinforced concrete walls, ceiling, and floor of the chamber are 1.22, 1.37, and 1.83 m, respectively.

The locations of existing Bunker 801 camera ports and the end of the FXR accelerator (see Fig. 3), all of which must be in the chamber, led to the selection of a chamber area of about 344 m^2 with an interior height of 9.5 m.

Figure 2. Plan view of the proposed Contained Firing Facility additions to Bunker 801.

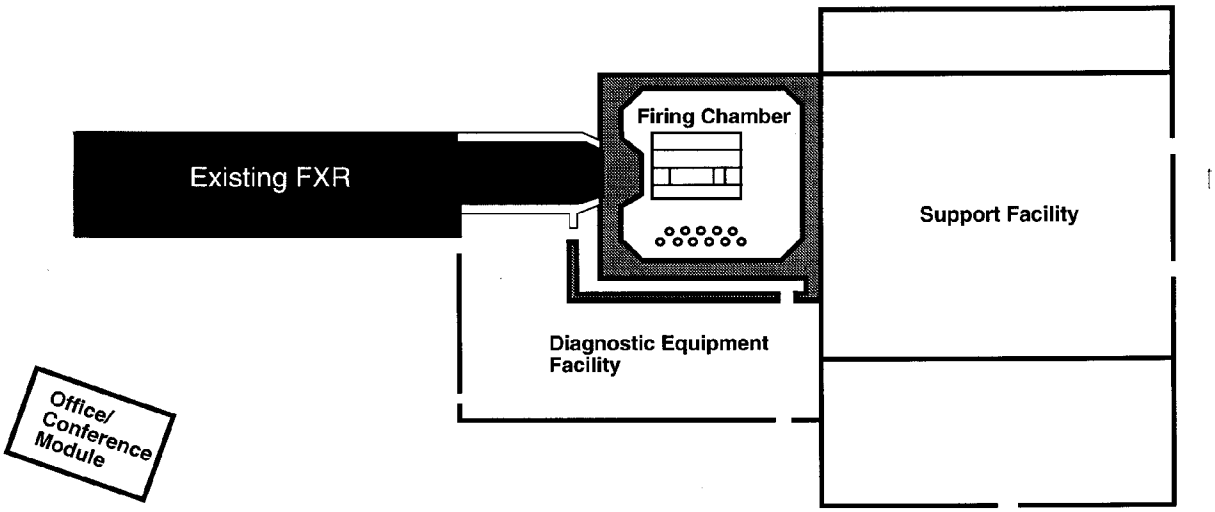

Figure 2. Plan view of the proposed Contained Firing Facility additions to Bunker 801.

The support facility (about 1543 m^2) provides a staging area for preparing the nonexplosive components of an experiment, equipment and materials storage, personnel locker rooms, rest rooms, and decontamination showers. It also houses the filters, scrubbers, and temporary waste-accumulation area for management of the waste products from testing.

The diagnostic equipment facility (about 576 m^2) will accommodate multiple-beam optical equipment to measure velocity-time histories from as many as 40 points on an explosively driven metal surface through 12 horizontal optical lines of sight (LOS's) into the firing chamber. These are in addition to 11 vertical optical LOS's from the existing Bunker 801 camera room situated below the chamber floor. This facility is similar in construction to the support facility and will also protect the personnel who may occupy this area during the explosives tests.

Figure 3. Plan view of the firing chamber, showing explosive mass limits.

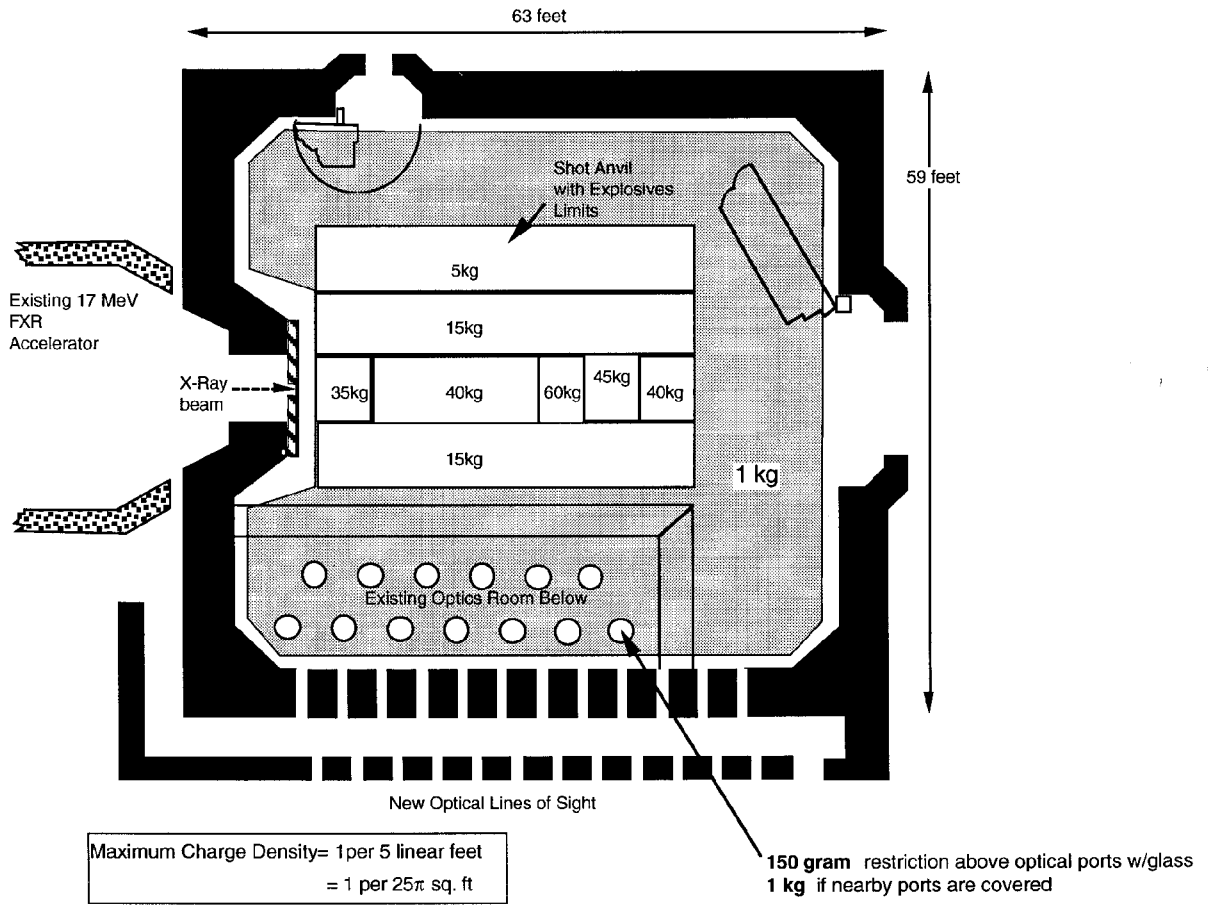

Figure 3. Plan view of the firing chamber, showing explosive mass limits.

Design Equivalency Criteria

The criterion for the design of the CFF is that it be able to elastically survive the blast effects from detonating a maximum of 60 kg of an energetic high explosive like PBX-9404. To design the chamber to survive this environment requires an equivalency conversion in the structural design process from energetic material to the standard (TNT). The equivalent TNT mass is based on a single worst-case equivalency factor (3 that conservatively (i.e., is based on current high explosives used at Site 300) encompasses all maximum effects from blast and quasi-static gas pressure. This factor β is defined as the largest ratio of the heats of detonation for energetic materials to that of TNT:

EQUATION 2

$$\beta = \frac{\Delta H_{\text{energetic material}}}{\Delta H_{\text{TNT}}} \approx 1.3 \quad . \qquad \textbf{(1)}$$

Due to variations in high-explosive charge initiation and the inaccuracies associated with construction materials, a safety factor of 1.2 is additionally specified[3] in the design equivalency process. The amount of TNT equivalent for structural design purposes is thus given by

EQUATION 3

$$\text{Mass of TNT design equivalent} = \beta \cdot 1.2 \cdot [\text{Desired HE operational mass}] \quad . \qquad (2)$$

For the CFF, this amounts to

$$\text{Mass of TNT design equivalent} = 1.3 \cdot 1.2 \cdot 60\text{kg} = 93.6 \text{ kg} , \qquad (3)$$

which is the basis for all the design calculations.

Environmental Considerations

"Contained firing" implies complete containment of all blast effects associated with the detonation of cased high-explosive materials. This includes discharges to the environment in the form of noxious gases, particulate matter (aerosolized and chunky), and impulsive noise produced from the detonation. While it is highly desirable to have a "zero discharge" criterion as a goal of the CFF project, it is recognized that, in reality, this is nearly impossible to achieve and excessively expensive to implement. Instead, the CFF project advertises a "near zero discharge" policy, whereby small discharges that are within all environmental regulations may occur from time to time over the estimated 40-year life of the facility. The distinction between an absolute zero discharge" facility and a "near zero discharge" facility is important socially and politically, in that small, environmentally acceptable, accidental discharges may result in closure of the facility if not planned for and advertised early in the design process.

The firing chamber is designed as a sealed structure to contain not only the very high-amplitude, short-duration impulsive shock pressures but also the much lower amplitude and longer quasi-static gas pressures that are typically associated with detonations of explosives in closed firing chambers. Anchored to the inside of the chamber surfaces is a thin, continuous, 12.7-mm-thick, mild-steel pressure liner. This pressure liner acts to seal and prevent passage of the detonation gases through the concrete walls, ceiling, and floor, which may develop structurally acceptable hairline cracks as the facility ages. All doors, optical LOS's, and other intrusions into the firing chamber (such as the FXR bullnose) will have seals that allow the firing chamber to function as a pressure vessel for containment of the noxious gases. After the gases cool down, blast dampers are opened, enabling ventilation fans to purge the chamber with fresh air. The exhaust gases are processed through HEPA (high-efficiency particulate absolute) filters and scrubbers before being released to the environment. Slight negative atmospheric pressures are maintained afterward in the firing chamber and the support facility to reduce the escape of unprocessed airborne hazardous particulates and gases to the environment. In contrast, during current open-air detonations, all of the gaseous by-products are released to the environment without being processed.

Solid wastes and shot-related debris are greatly diminished and can be collected and disposed of as low-level radiated waste or as mixed waste, as appropriate. In conjunction with the management of these solid wastes, a reactive-waste certification program is being developed at LLNL. An internal, closed, water, wash-down system is planned that recirculates water spray within the chamber and filters out dust and particulates in the form of sludge. The CFF project will accomplish aggressive waste minimization by reducing the total solid wastes to an estimated one-tenth of what is currently generated today.

Blast-Effects Supplemental Testing

After review of the CFF CDR, a few critical blast-effects design issues were identified that, due to their imprecise nature, would benefit from further investigation. A program primarily based on empirical blast effects testing was formulated in each of the following four areas:

Shrapnel mitigation

Global structural response

Qualification and acceptance testing

Close-in shock loading.

The focus of this report is the close-in shock loading that will occur on the floor of the proposed firing chamber. The rationale for each of the testing programs is described briefly as follows:

Shrapnel Mitigation
High-velocity fragments from cased explosives could do significant damage to the pressure

liner in the firing chamber and thereby compromise the containment and sealing of hazardous gases and particulates. A series of actual worst-case shrapnel-producing experiments at Site 300 were monitored and documented[5] to evaluate various general-purpose shrapnel-protection schemes. The resulting design, as shown in Fig. 4, is a replaceable, general-purpose, multilayer, protection scheme to be installed on the inside surfaces of the firing chamber. As a result of the testing, three important design modifications to the conceptual design could be realized:

FIGURE 4. SHRAPNEL-MITIGATION TESTING APPARATUS.

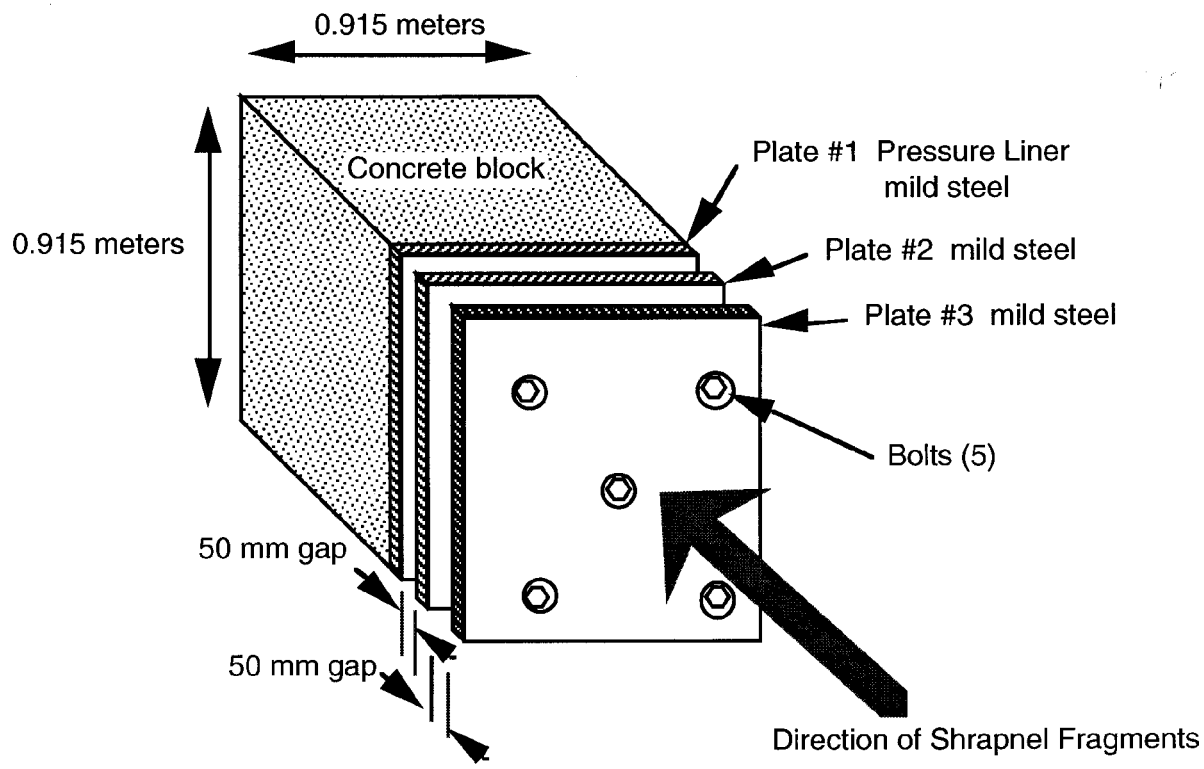

Figure 4. Shrapnel-mitigation testing apparatus.

Additional local shielding would be required on an as-needed basis near those experiments that produce material with a directional nature (e.g., shaped charges). Addition of localized shielding permits the overall general-purpose shielding to be thinner, resulting in a cost saving.

Providing general-purpose shielding made from mild steel instead of armor plate, since mild steel is roughly half the cost and provides about 85% of the penetration resistance of armor plate.

Using multilayer technology, whereby thinner shrapnel-mitigation plates are separated by air spaces, thereby permitting the total thickness of shielding to be reduced and facilitating replacement and repair.

Total Structural Dynamic Response

Recent experience from qualification testing of the contained firing vessels in the High-Explosives Applications Facility (HEAF)[6] at the LLNL main site in Livermore indicates that the highest measured strains occur after the shock loading has passed and are due primarily to the vibrational modes of the structure that are excited by the impulsive nature of the detonation. Figure 5 shows a quarter-scale model of the firing chamber instrumented with strain gages, pressure transducers, and temperature gages. The quarter-scale model will be subjected to various scaled charge equivalents from 25% to 125% to verify that all of the resulting strains in the structure are within elastic limits. The quarter-scale model, if proved successful, will then be

Figure 5. Quarter-scale model of the firing chamber.

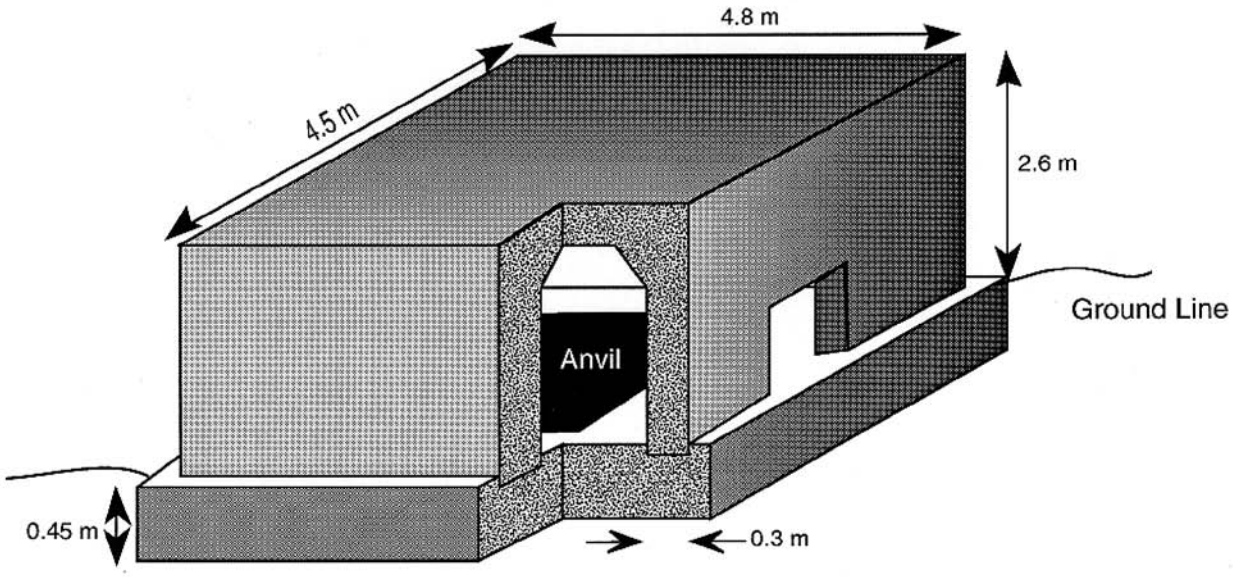

Figure 5. Quarter-scale model of the firing chamber.

used after the CFF is constructed as a testing prototype to try out quarter-scale versions of future risky experiments that might cause permanent structural damage to the full-size firing chamber.

Qualification Testing

After the CFF is constructed but before it is used for conducting normal experiments, a series of qualification tests will be performed in the firing chamber to test it and the support systems. Explosives tests that produce up to 125% of the chamber pressure capacity are required by Laboratory policy[7] to further ensure that the facility has been safety constructed and that it meets or exceeds the original design criterion of totally elastic response. As with the quarter-scale model of the firing chamber, the actual firing chamber will be instrumented with

permanent gaging to assess the effects of the required qualification tests.

The permanent strain gages and pressure transducers can then be monitored at any time during detonations over the anticipated 40-year life of the airing chamber to ensure safe and reliable operation.

Close-in Shock Loading

The highest unit shock (blast) loading that the CFF must withstand will occur on the floor just below the explosive charge location. Currently, due to diagnostic requirements of the FXR and the desired operational optical lines of sight, this distance is 1.22 m. This results in an extremely close-in ($Z = 0.66$ ft/lb$^{1/3}$) blast loading on the reinforced concrete floor of the chamber. The remainder of this report describes the blast testing and computer analysis conducted on a quarter-scale model of the preliminary floor design.

Close-in Blast-Loading Experiments-Floor Section Testing

Introduction

Historically, floor damage due to close-in loading has been a common problem for other blast chambers within the DOE/DoD. Given this, the close-in blast loading on the chamber floor is considered to be one of the critical design issues associated with the proposed CFF. To evaluate the preliminary CDR floor design, it was first proposed that a replica scale model of the firing chamber floor be tested. Since the close-in blast loading is anticipated to be highly localized, the focus of our testing was narrowed to only a section of a replica scale floor situated directly below the high explosive. This "cookie-cutter" concept of testing just a section of the replica scale model of the floor section was then verified by a DYNA-3D computer analysis as a legitimate substitute for constructing and instrumenting a complete replica scale model of the floor. It was further recognized that all blast reflections from the ceiling and walls would be absent, as would be the quasi-static gas loading due to confinement. These additional loadings would be present in a replica scale model of the complete firing chamber as a future testing project.[7]

Floor Section Description

A 1/4-scale model of the floor was chosen as a compromise between modeling scalability and cost. Figure 6 shows a cross section of the cookie-cutter floor section, complete with equivalent structural reinforcing. The floor section consisted of a rectangular 3- x 3- x l .5-ft-thick,

Figure 6. Floor section cut-away pictorial.

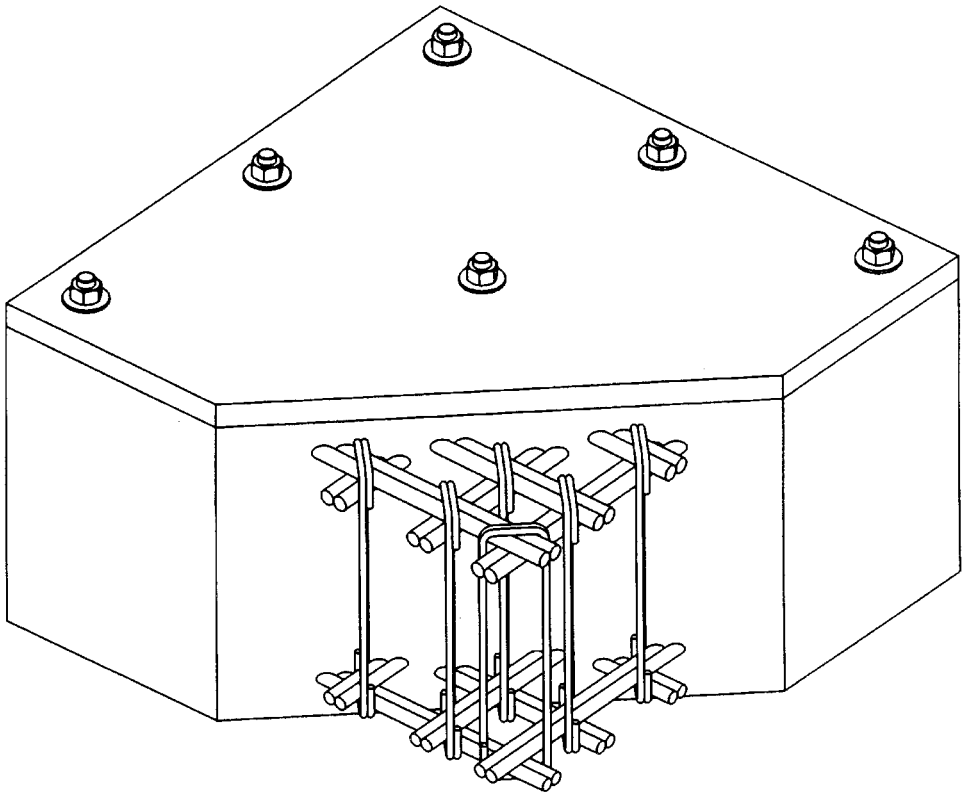

Figure 6. Floor section cut-away pictorial.

steel-reinforced, cast concrete block set on a compacted base foundation of 12 in. of soil with a dry density of 104 lb/ft^3 and an additional 8 in. of class II aggregate base rock with a dry density of 142 lb/ft^3 (see Ref. 9). A sample of the compacted base foundation was measured at 91.8% relative compaction.[10]

A 1.5-in.-thick, mild-steel plate was used to model the 6-in.-thick shot anvil on the top of the block. The shot anvil was clamped to the floor section using nine, 1-in., 8-UNC x 9-in., grade 2 bolts torqued to 200 ft-lb. Concrete with a minimum compressive strength of 6000 psi was used per the CDR. Actual test data[11] showed the strength to be an average of 6600 psi at 28 days. No attempt was made to scale the aggregate size, which was assumed to have a minor effect. The steel reinforcing consisted of grade 60 rebar, with pairs of #7 bar for the upper mat and pairs of #6 bar for the lower mat, and with stirrups of #3 bar vertically between the mats. The spacing between the upper and lower mats was nominally set to 15 in. Exact replica scaling could not be achieved by using conventional rebar sizes. Instead, equivalent scaling was used by adjusting the horizontal rebar spacing to 6 in. to preserve the CDR ratio of rebar to concrete on a per-volume basis. To maintain good contact between the bottom of the anvil and the concrete, the floor section assembly was cast upside down upon the anvil. The

assembly was later inverted after the concrete had cured for 28 days.

Nineteen blast tests ranging from scaled distances of 1.14 ft/lb$^{1/3}$ (25%) to 0.57 ft/lb$^{1/3}$ (200%) were performed on the strain-gaged floor model. Spherical, bare, center-detonated C4 high explosive was used to provide the blast loading on the floor section. For all 19 tests, the charge was supported by lightweight strings such that the center of the charge was 12 in. above the top surface of the shot anvil.

Instrumentation

The floor section instrumentation consisted of 14 strain gages embedded in the concrete, on the reinforcing bars, on the hold-down bolts, and under the anvil surface to measure the resulting blast-induced strains. The exact strain-gage locations and model numbers are shown on drawing (AAA-92-106176-OA in Appendix B) and are summarized in Table 1.

Table 1. Strain-gage instrumentation.

Gage location	Gage number
Center bolt	Bolt 1
Side bolt	Bolt 2
Corner bolt	Bolt 3
Center concrete Z	sg4
Top rebar X	sg5
Top rebar Y	sg6
Lower rebar X	sg7
Lower rebar X	sg8
Upper concrete X	sg9
Lower concrete X	sg10
Anvil X	sg11
Anvil Y	sg12
Lower concrete Y	sg13
Center stirrup Z	sg14

Table 1. Strain-gage instrumentation.

Strain gage no. 6 on the top rebar was lost during construction of the floor section and was not recorded during the testing. Typical weld-on rebar and concrete embedment strain-gage installations are depicted in Figs. 7 through 9. Figure 10 shows the wooden formwork used to contain the concrete that surrounded the steel reinforcing cage. Figure 11 shows the completed 1/4-scale floor section prior to testing at the 25% explosive weight level.

Figure 7. Weld-on strain gages: (1) spot-welded to ground surface of rebar; (2) after protective covering was applied.

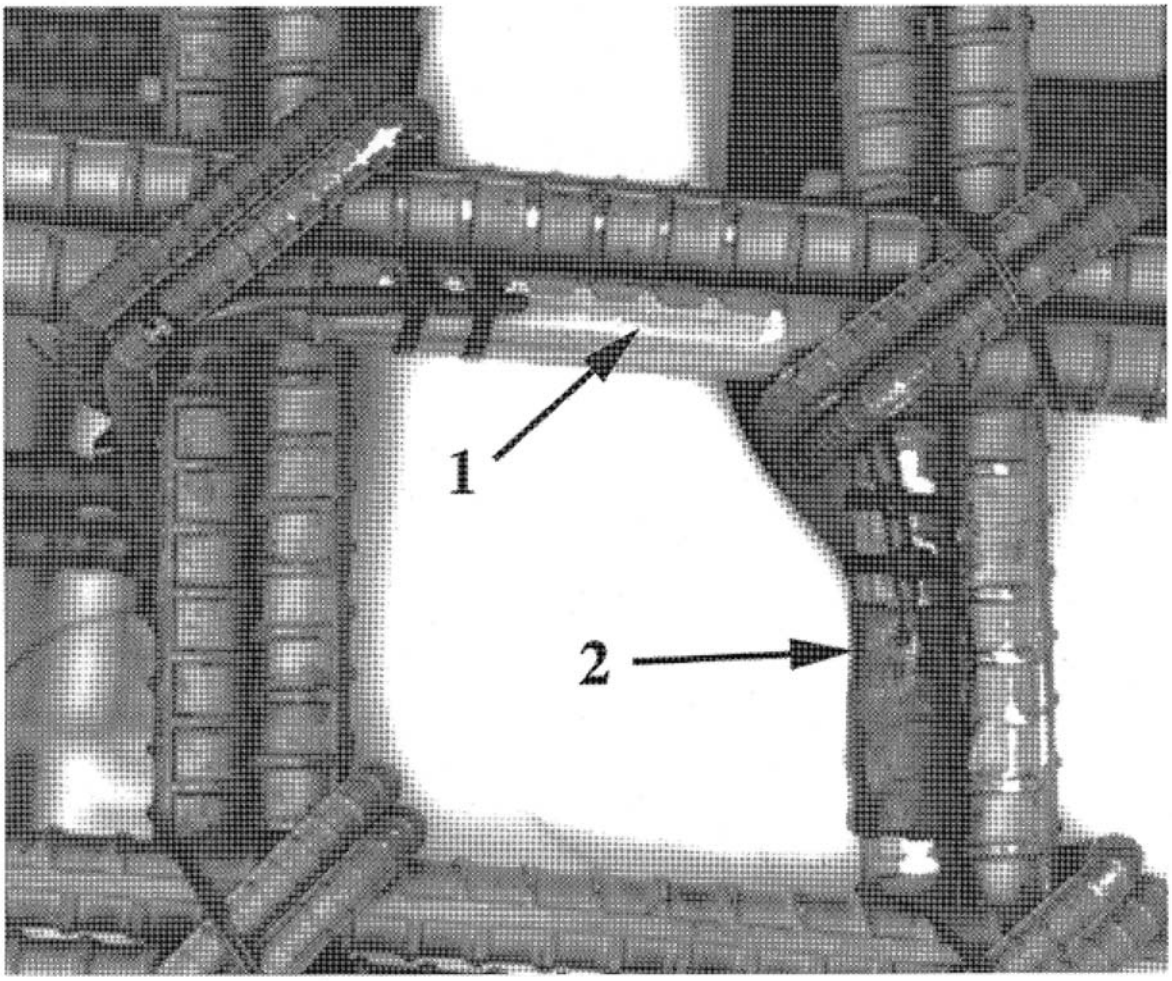

Figure 7. Weld-on strain gages: (1) spot-welded to ground surface of rebar; (2) after protective covering was applied.

Figure 8. Concrete embedment gages mounted orthogonally in the same plane as the lower rebar mat.

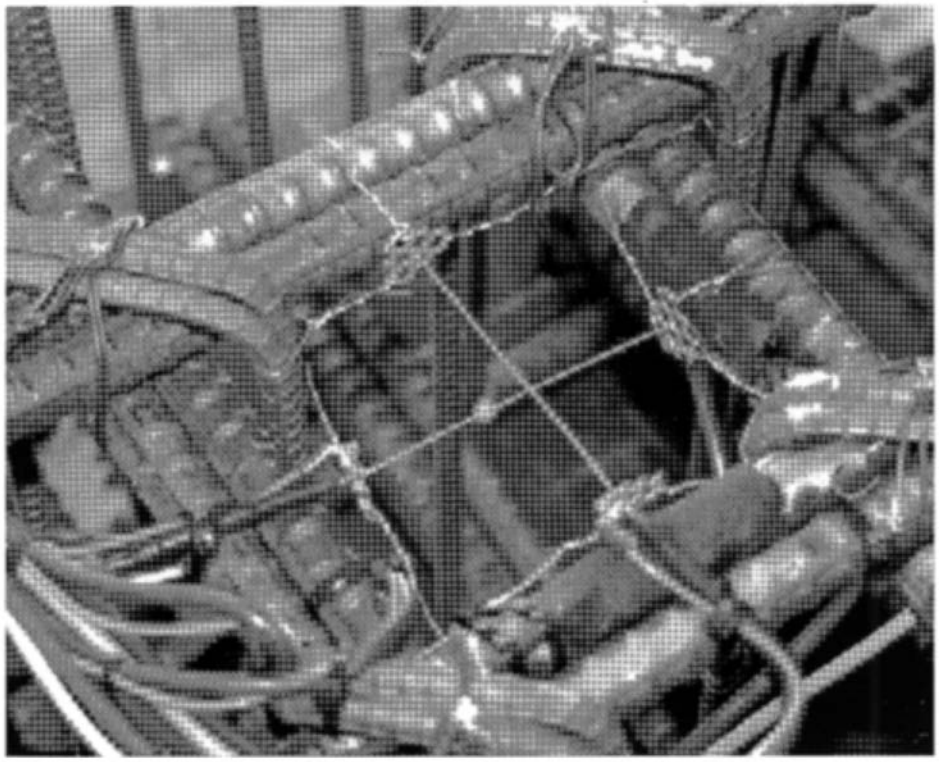

Figure 8. Concrete embedment gages mounted orthogonally in the same plane as the lower rebar mat.

Figure 9. Inverted rebar cage in final stages of instrumentation installation. Note concrete embedment gage (#4) suspended in center of cage.

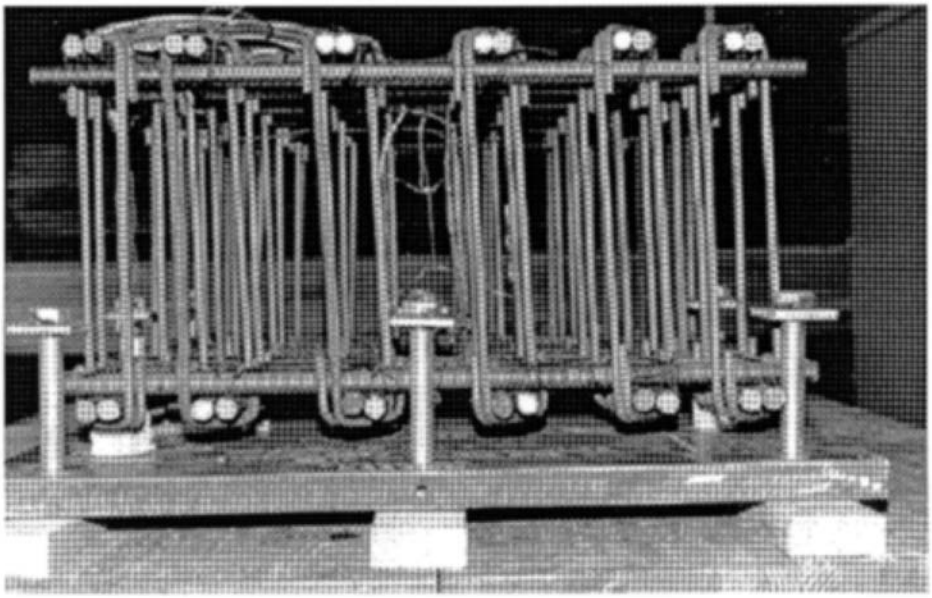

Figure 9. Inverted rebar cage in final stages of instrumentation installation. Note concrete embedment gage (#4) suspended in center of cage.

Figure 10. Wooden formwork used to contain the 6000-psi concrete that surrounded the steel reinforcing cage. Concrete was placed carefully by hand to protect the delicate concrete embedment strain gages from damage during the pour.

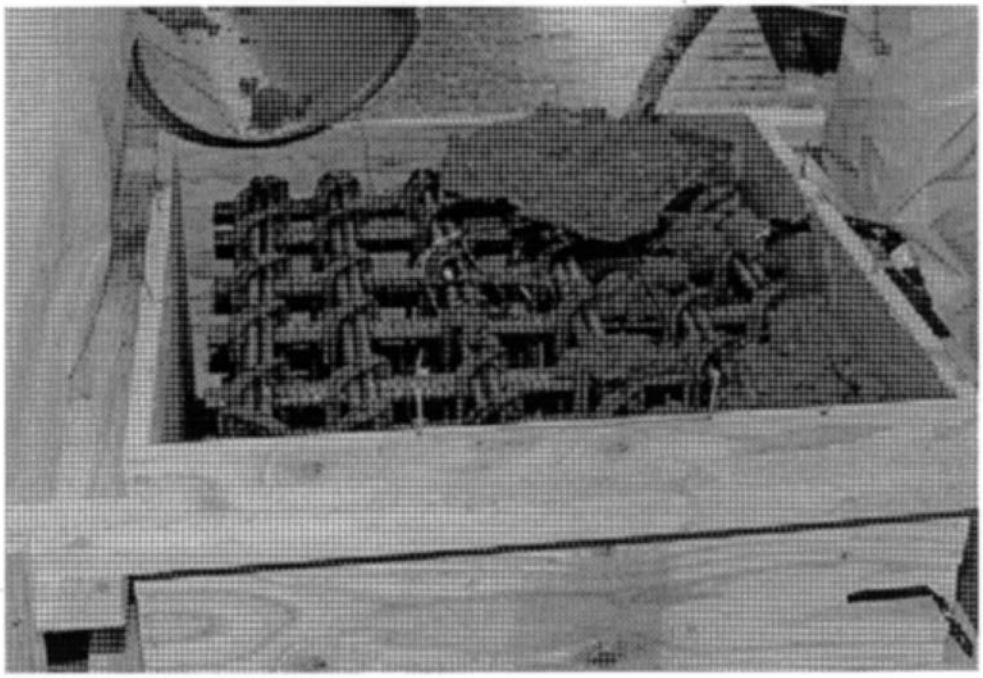

Figure 10. Wooden formwork used to contain the 6000-psi concrete that surrounded the steel reinforcing cage. Concrete was placed carefully by hand to protect the delicate concrete embedment strain gages from damage during the pour.

Figure 11. Completed 1/4-scale floor section prior to testing at the 25% explosive weight level.

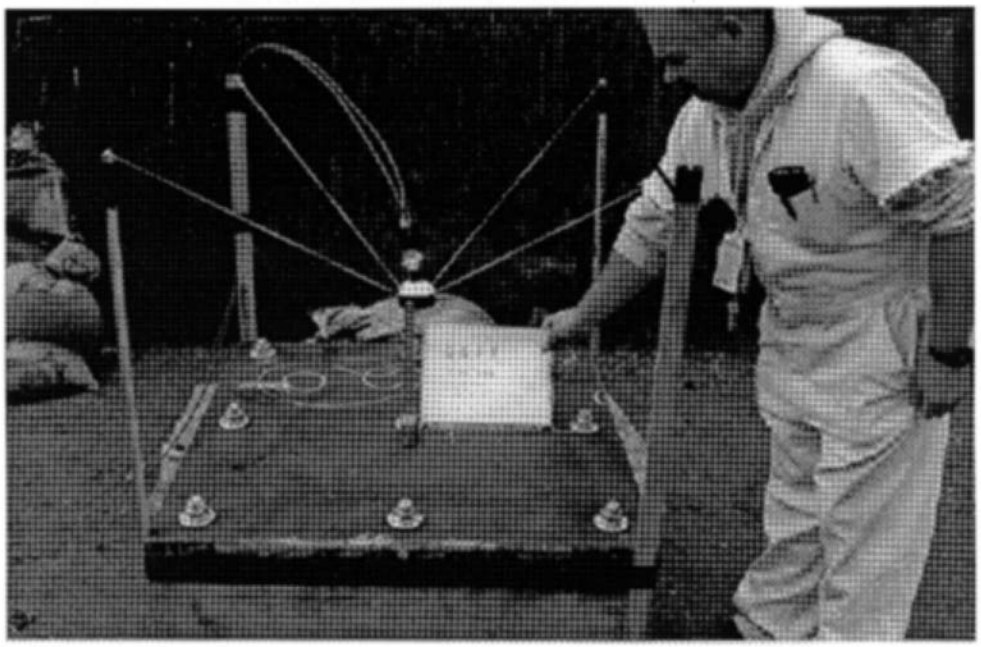

Figure 11. Completed 1/4-scale floor section prior to testing at the 25% explosive weight level.

Empirical Results

The worst-case measured strains, as recorded from all 19 tests, are summarized in Tables A1 and A2 of Appendix A. For tests 1 and 2 at the 25% level, all strains were below the yield points at all locations. As testing proceeded at the 50% level, gages 4 and 10 both exceeded the dynamic yield, indicating unacceptable tensile strains vertically in the concrete as well as unacceptable bending at the outermost lower rebar. Testing proceeded up through 125%, with two tests at each shot level. Since there were no visible cracks on the outside of the floor section and the block was still intact, testing proceeded (despite higher-than-yield strain readings in the concrete) to perform repetitive shots at 125% on the assumption that the floor was cracked internally and that it might take many shots for a crack to propagate to a visible outside surface.

After the fifth shot at 125%, visible hairline cracks appeared that ran from the top to the bottom of each side of the floor section, indicative of excessive bending (Fig. 12). A sixth shot was then fired at 125% to see if the strains in the cracked floor section would increase or remain the same. They remained about the same, even though the floor was visibly cracked (Fig. 13).

Based on the maximum measured strains in Tables Al and A2, the corresponding maximum tensile and compressive stresses have been calculated and are shown in Tables A3 and A4, respectively. Material properties listed in Table 2 were used to calculate the maximum stresses from the measured maximum strains. To access and evaluate the original nonyielding criteria, the safety factors for tensile and compressive yielding based on the Table 2 properties were calculated and are listed in Tables AS and A6, respectively. Safety factors less than l indicate yielding and are shown in bold for graphical comparison. It is clear from Table AS that tensile failures in the concrete began at the 50% shot level and continued up through the higher shot levels.

Figure 12. Typical vertical fractures on each side that became evident after the fifth test at the 125% explosive weight level.

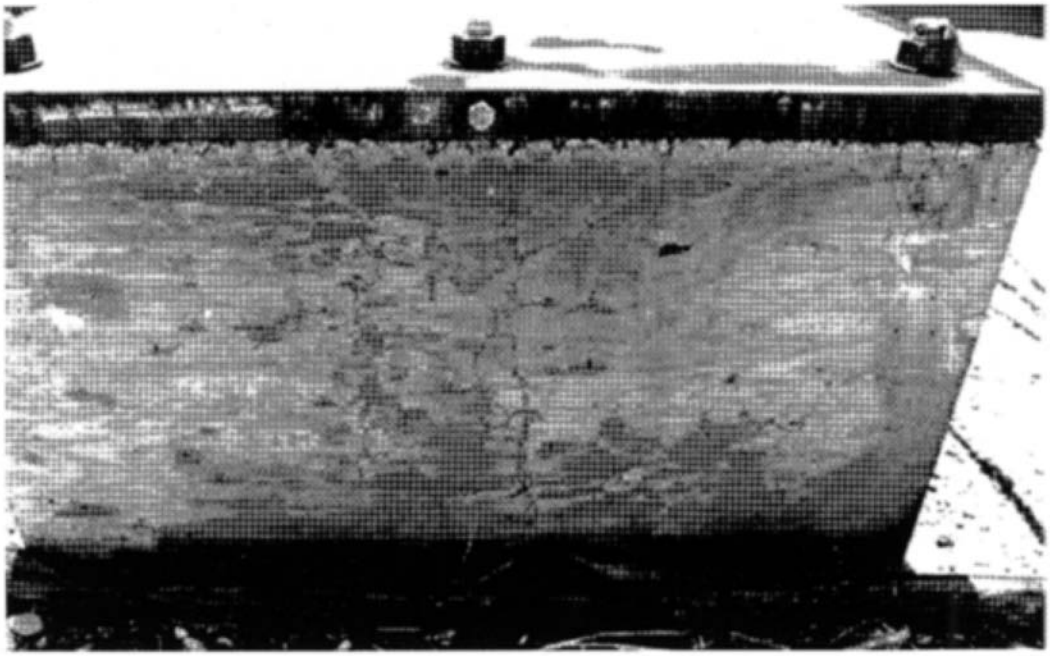

Figure 12. Typical vertical fractures on each side that became evident after the fifth test at the 125% explosive weight level.

Figure 13. Visible cracking on the bottom of the floor section block while it was hoisted on its side for inspection.

Figure 13. Visible cracking on the bottom of the floor section block while it was hoisted on its side for inspection.

Table 2. Material properties and acceptable strain levels.

Category	Elastic modulus (10^6 psi)	Microstrain at yield	
		Tensile	Compressive
Bolts	30.00	1200	1200
Rebar	29.00	2069	2069
Concrete	4.68	125	1410
Anvil	29.00	1241	1241

Table 2. Material properties and acceptable strain levels.

BLAST-ATTENUATION EXPERIMENTS

Before the two planned shots at 200%, the original planned testing was augmented by introducing five different blast-attenuation systems between the high-explosive charge and the shot anvil. These attenuation systems were quickly put together and tested at the 125% level in an attempt to limit the amount of shock transmitted to the floor and thereby accommodate the CFF design criterion of totally elastic response. Even though it was determined that the floor section was cracked and had continued to yield with each shot, it was judged that the floor section was still usable and could provide fairly consistent results. A sixth shot at 125% (test #12) was performed to verify this observation and was used as the basis for comparing the various blast-attenuation systems.

Each of the five blast-attenuation systems consisted of different crushable materials protected from the fireball by a metal inertial plate. The criterion for each system was that they should be simple, provide blast attenuation, and be reusable to minimize shot waste. Table 3 describes the properties of each attenuation system tested. It is important to note that, for all 19 tests, the distance between the center of the high-explosive charge to the top of the shot anvil in the floor was maintained at 12 in., regardless of the attenuation system or lack of it.

The following discussion describes the results of each type of blast-attention system used in terms of its ability to attenuate the measured strains in the floor section. The basis for evaluation is the safety factor for tensile yielding (SF_y), as listed in Table A5 of Appendix A. All attenuation systems appear to be acceptable from the point of view of compressive strain safety factors, as listed in Table A6.

Table 3. Description of blast-attenuation systems tested.

Test No.	Crushable material	Attenuation layer Thick. (in.)	Width (in.)	Length (in.)	Inertial mass (A36 steel) Thick. (in.)	Width (in.)	Length (in.)
13	Open-cell polystyrene foam (0.05 g/cm^3)	1	14	24	0.5	24	24
14	Neoprene flat gasket (8 pads)	0.5	6	3 (4) 2 (4)	0.5	24	24
15	High-temperature silicone-rubber sheet	0.5	24	24	0.5	24	24
16, 18	Rubber brush door mat	0.625	24	24	1.0	24	24
17	Vinyl slotted-pyramid-top mat	0.4375	24	24	1.0	24	24
19	High-temperature silicone-rubber mat (5 pads)	0.5	6	6	1.0	24	24

Table 3. Description of blast-attenuation systems tested.

Open-Cell Polystyrene Foam

Used for test #13, the attenuation material consisted of eight pieces of 0.05g/cm^3 open-celled polystyrene foam. When pieced together, the foam completely filled the region between the anvil and the inertial mass. Compared to a bare anvil, the foam system greatly reduced the peak strains to generally acceptable levels. The only exception was detected by gage #10, which produced an improved but still unacceptable safety factor (SF < 0.7). Additionally, the foam was not reusable; for these reasons, it was deemed unacceptable.

Neoprene Flat Gasket

Used for test #14, this 0.25-in.-thick material was placed in two layers to give a total thickness of 0.5 in. Due to limited availability, it was used in eight discrete positions under a 0.5-in.-thick inertial mass. The neoprene flat gasket material also greatly reduced the recorded peak strains, except for gages #4 and #10, which produced unacceptable yield safety factors of 0.4 and 0.7, respectively. For this reason, the neoprene flat-gasket attenuation system was judged unacceptable.

High-Temperature Silicone Rubber

Used as a solid sheet for test #15 and again as five discrete pieces for test #19, this material (Fig. 14) proved to be extemely tough and durable. However, this was the only attenuation material that failed by actually amp1ifying the peak strains measured in the floor. Strain gages l, 9, 10, and 13 produced unacceptable yield safety factors (SF < l) in tension for tests at 125% and 200%. For these reasons, the flat high-temperature silicone material was judged unacceptable.

Figure 14. Samples of three blast-attenuation materials (L to R): vinyl slotted-pyramid-top mat, rubber-brush door mat, high - temperature silicone elastomer sheet.

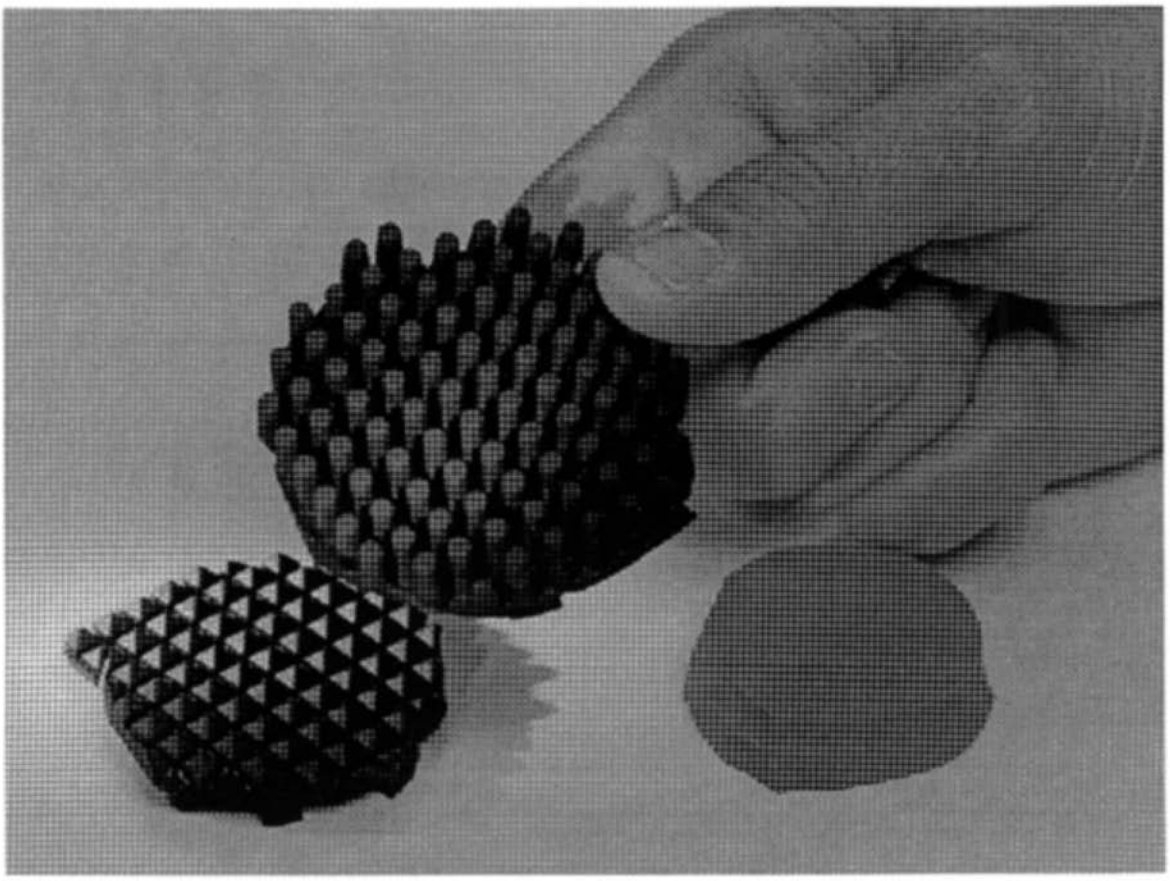

Figure 14. Samples of three blast-attenuation materials (L to R): vinyl slotted-pyramid-top mat, rubber-brush door mat, high-temperature silicone elastomer sheet.

Vinyl Slotted-Pyramid-Top Mat

Used for test #17, this material (Fig. 14) is basically a low-cost door mat with geometric molded features on its surfaces. One side of the mat has short cylinders projecting from the mat, while the other side has small pyramid-shaped protrusions, as shown in Fig. 14. Like most of the other attenuation materials, the vinyl mat greatly reduced the peak tensile strains, except for strain gages 4, 9, and 10, which all produced safety factors for tensile yield below 1.0. For this reason, the vinyl mat was also judged unacceptable.

Rubber-Brush Door Mat

Used for tests #16 and #18, this material (Fig. 14) is a low-cost, rubber-brush, door-mat

material with many slender rubber cylinders projecting from its base. For test #16 at 125%, this was the only material that prevented yielding at all of the strain-gage locations. With the addition of this b1ast-attenuation system, all of the measured strains at the 125% shot level were reduced to levels below yield. For this reason, the rubber-brush door-mat system (shown in Figs. 15-17) was judged to be acceptable.

Figure 18, a typical plot for the vertical concrete stresses (gage #4) at 125%, shows a stress-time history which indicates that the rubber-brush door-mat attenuation system effectively reduces the tensile shock wave to an acceptable level. Figure 19 shows that the resulting tension

Figure 15. Placement of rubber brush door mat on top of anvil firing surface in preparation for test #16 at 125%.

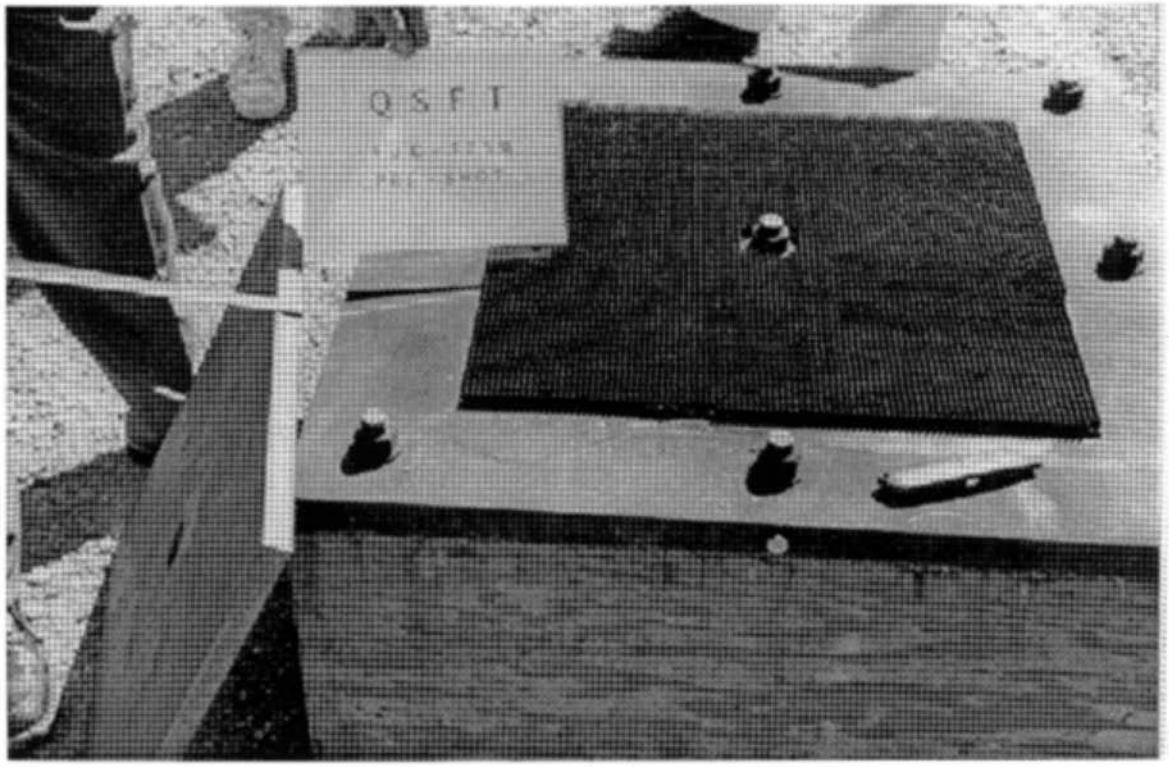

Figure 15. Placement of rubber brush door mat on top of anvil firing surface in preparation for test #16 at 125%.

Figure 16. Blast-attenuation system consisting of the inertial reaction mass plate and rubber-brush door mat in place on the anvil just prior to firing test #16 at the 125% explosive weight level.

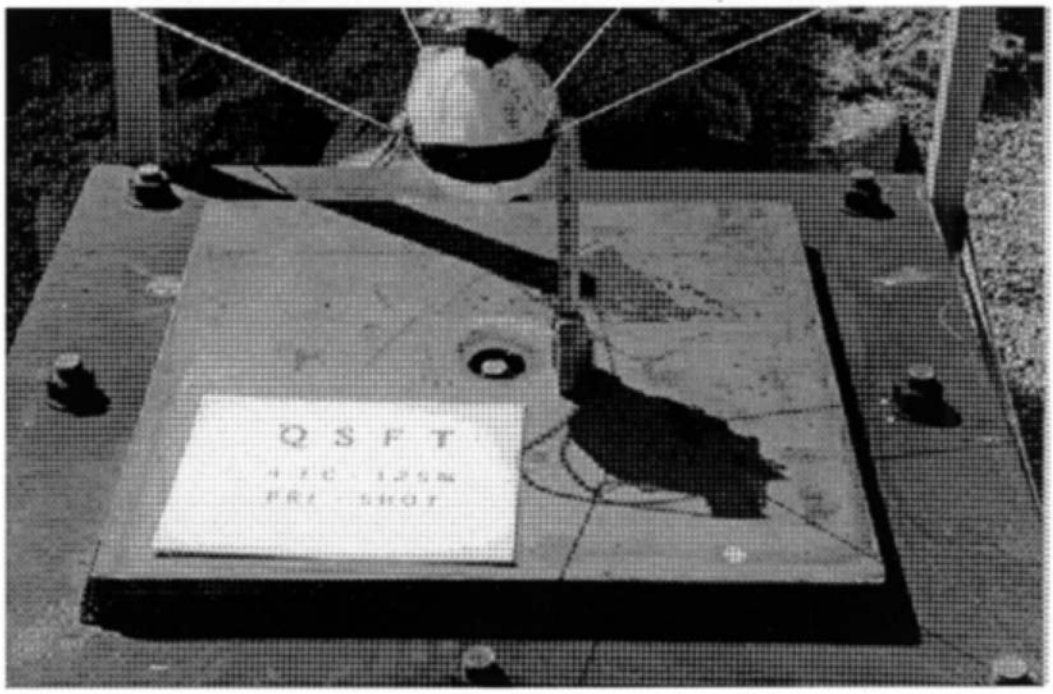

Figure 16. Blast-attenuation system consisting of the inertial reaction mass plate and rubber-brush door mat in place on the anvil just prior to firing test #16 at the 125% explosive weight level.

Figure 17.
Location of blast-attenuation system immediately after firing test #16.

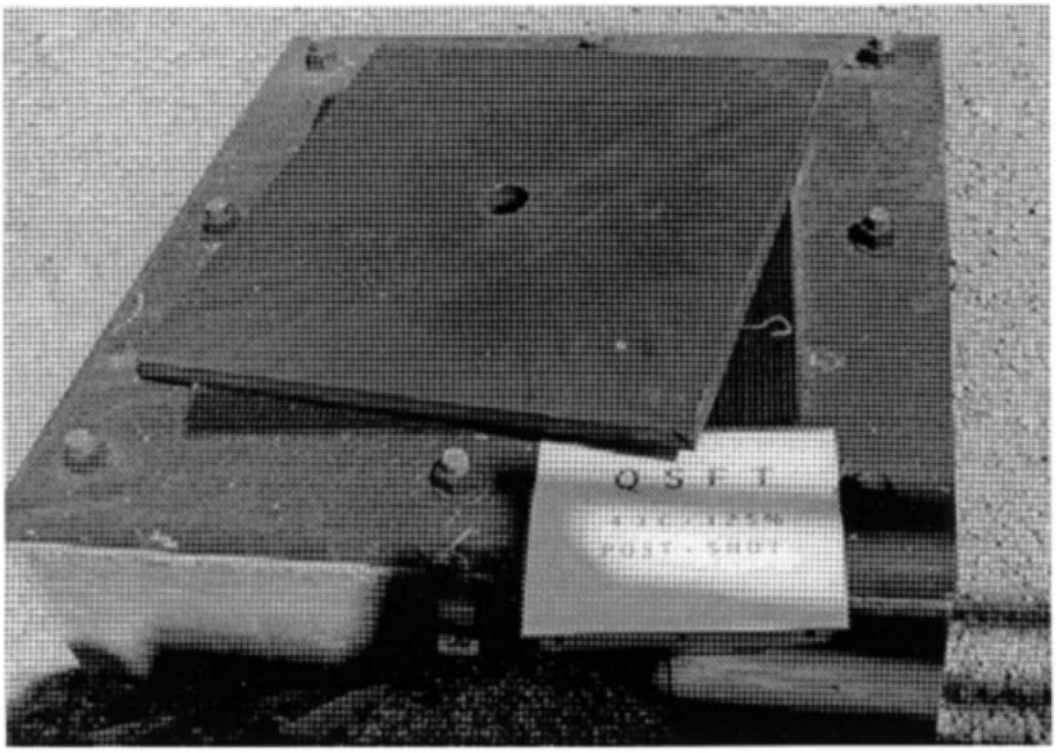

Figure 17. Location of blast-attenuation system immediately after firing test #16.

FIGURE 18. VERTICAL CONCRETE STRESS (GAGE #4) IN THE CENTER OF THE BLOCK AT 125% SHOT LEVEL FOR (a) BARE CHARGE (TEST #12) AND (b) REDUCED BY ADDITION OF RUBBER-BRUSH DOOR-MAT BLAST-ATTENUATION SYSTEM (TEST #16)

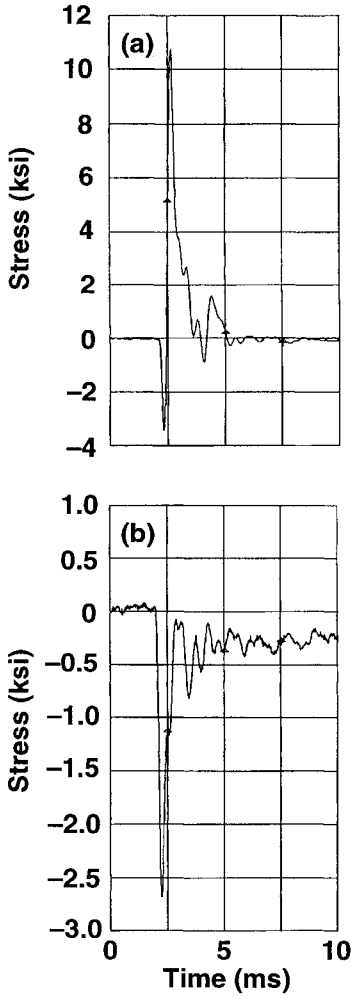

Figure 18. Vertical concrete stress (gage #4) in the center of the block at 125% shot level for (a) bare charge (test #12) and (b) reduced by addition of rubber-brush door-mat blast-attenuation system (test #16).

Figure 19. Stress due to bending for concrete gage (#13) in the bottom of the block at 125% shot level for (a) bare charge (test #12) and (b) reduced by addition of rubber-brush door-mat blast-attenuation system (test #16)

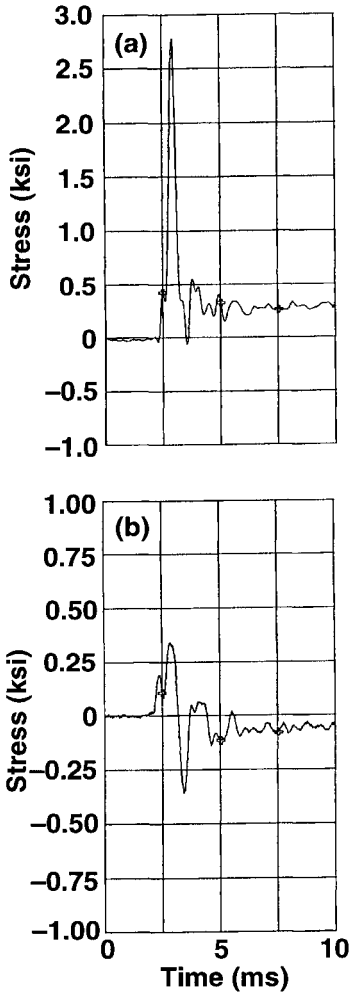

Figure 19. Stress due to bending for concrete gage (#13) in the bottom of the block at 125% shot level for (a) bare charge (test #12) and (b) reduced by addition of rubber-brush door-mat blast-attenuation system (test #16).

from bending loads caused by the incident shock wave also is reduced to acceptable levels by the attenuation system.

Dynamic Computer Analysis

The following results represent an application of the latest finite-element technology for analyzing a structure that is normally designed by codified single-degree-of-freedom methods. Prior to testing, DYNA-3D, an explicit, large-deformation, finite-element computer program was selected as a tool to try to predict stresses resulting from the dynamic response

of the CFF floor. This was done for three reasons:

To check the validity of the equivalent replica scaling used to model the CDR preliminary floor design.

To validate the cookie-cutter concept of testing only a small section of a scale model of the floor.

To check the strength of the concrete in the CDR preliminary design to see if it met the design criterion of dynamic elastic response without yielding.

Two DYNA models were created for evaluating the proposed replica scaling of the floor. One model consisted of the full-size CDR floor, whereas the second model was for an equivalent replica 1/4-scale model floor. By symmetry, only 1/4 of each geometry was meshed to save computational time. In a comparison of eight model parameters, both models agreed closely, with an average difference of 9.5% lower stresses in the 1/4-scale model's favor. The 1/4-scale floor model predicted slightly higher stresses only for the lower concrete in axial tension and the average normal stress. Therefore, the equivalent replica scale model was judged to be acceptable.

To verify the cookie-cutter approach, a third DYNA model was created for the 1/4-scale floor section. Compared to the full 1/4-scale floor, the cookie-cutter floor predicted similar stresses due to the impulsive loading but also predicted slightly exaggerated bending in the lower floor section. This was attributed to increased reflections as a result of the smaller cookie-cutter design. Overall, the cookie cutter was judged to conservatively represent the full 1/4-scale floor.

The results of the full-size floor analysis indicate that the floor appears to be susceptible to damage for concrete with a 6-ksi compressive strength. A uniaxial compressive strength of 7 ksi was estimated[12] to be necessary to prevent compressive damage and to ensure completely elastic response.

Observations and Conclusions

For close-in, localized blast loading on the floor, testing only a small scaled section of the floor located vertically below the explosive charge was shown computationally to be valid in lieu of testing a complete scaled floor.

Normally in reinforced-concrete design, the tensile strength of the concrete is ignored, and the reinforcing carries all of the tensile load. When this happens, the concrete will crack if its dynamic tensile strength is exceeded, and this is acceptable for some designs. For the two-way bending that occurs in the floor of the present conceptual design, long-term damage (cracking) of the concrete in the floor is predicted to occur from the planned extemely close-in blast loading on the floor. Tensile strains recorded from the 125% shot levels were 10 times the allowable dynamic tensile yield for the specified concrete. This is a concern if the cracks

continue to open up or grow with time and allow excessive bending and thus yielding of the reinforcing. All other measured strains in the reinforcing and anvil appear to meet the CFF design criterion of elastic response.

Various simple blast-attenuation systems were investigated, which led to a system that protected the concrete in the floor from tensile failures and thereby enabled the conceptual floor design to meet the CFF design criterion of elastic response. Average tensile strain improvements of 500% and average compressive strain improvements of 50% were realized, as summarized in Tables 4 and 5.

The vertical visual cracks in the floor as shown in Fig. 13 may have been caused in part by localized tensile loading that resulted when the anvil rebounded upward after being hit by the initial downward blast-induced shock. The spacing between anchor bolts should be decreased to reduce and thus spread out the tensile rebound forces more uniformly throughout the floor.

Table 4. ***Tensile*** **strain improvement for yielding resulting from attenuation at 125% explosive shot level.**

		Average safety factor for yield		
	Yield strength	Unattenuated	Attenuated	Improvement
Category	(psi)	(Test #12)	(Test #16)	by category (%)
Bolts	36,000	2.9	12.6	334
Rebar	60,000	3.1	31.4	913
Concrete	585	0.2	1.7	750
Anvil	36,000	6.6	6.6	0
		Average *tensile* strain improvement: 500%		

Table 4. Tensile strain improvement for yielding resulting from attenuation at 125% explosive shot level.

Table 5. *Compressive* strain improvement for yielding resulting from attenuation at 125% explosive shot level.

Category	Yield strength (psi)	Average safety factor for yield: Unattenuated (Test #12)	Average safety factor for yield: Attenuated (Test #16)	Improvement by category (%)
Bolts	36,000	10.9	20.8	91
Rebar	60,000	22.3	21.5	–4
Concrete	6,600	10.0	9.6	–4
Anvil	36,000	5.4	11.6	115

Average *compressive* strain improvement: 50%

Table 5. Compressive strain improvement for yielding resulting from attenuation at 125% explosive shot level.

Acknowledgment

This work was performed under the auspices of the U.S. Department of Energy by the Lawrence Livermore National Laboratory under Contract No. W-7405-Eng-48.

Footnotes and References

1. *Site 300 Contained Firing Facilities-Conceptual Design Report*, U.S. Department of Energy Project Number 94-SAN-LLN-02, prepared by Holmes & Narver Architects-Engineers, Sept. 1992.

2. The design of this facility is governed by DOE requirements and regulations found in DOE 5481.1B, DOE 5430.1A, DOE 6430.1A, DOE/AD-0006/1, DOE/EV-0043, DOE/EV-06194 *(DOE Explosives Safety Manual)*, DOE/NEPA, and 10CFR Part 435 *(Energy Conservation Report)*.

3. Composition of HMX: octahydro- 1,3 ,5,7-tetranitro- 1,3,5 ,7-tetrazocine.

4. *Structures to Resist the Effects of Accidental Explosions*, Joint Departments of the Army, the Navy, and the Air Force, TM5-1300/NAVFAC P-397/AFR 88-22, Nov. 1990.

5. J. W. Pastrnak, C. E Baker, and L. E Simmons, *Shrapnel Protection Testing in Support of the Proposed Site 300 Contained Firing Facility*, Lawrence Livermore National Laboratory, UCRL-ID-110732 (1992).

6. The High-Explosives Application Facility can detonate up to 10 kg of high explosive in stainless-steel firing vessels.

7. *Health & Safety Manual*, Lawrence Livermore National Laboratory, Livermore, CA, M-010, Jan 1990, chapter 6.26.

8. J. W. Pastrnak, 1/4 Scale Model Project Plan (June 18, 1993).

9. *Moisture Density Relations Test Report*, Consolidated Engineering Laboratories, Pleasanton, CA, report PFN # 812-93001(1992).

10. *Soils Inspection Report*, Consolidated Engineering Laboratories, Pleasanton, CA, report PFN #812-93001(1992).

11. *Concrete Compression Test Data*, Consolidated Engineering Laboratories, Pleasanton, CA, report PFN # ENV-91015 (1992).

12. G. Kay and S. Govindjee, "Site 300 Contained Firing Facility Floor Analysis," LLNL interdepartment memo to J. Pastrnak, Nov. 5, 1992.

Appendix A

TABLE A1. Quarter-Scale Floor Tests (QSFT) Maximum Tensile Strain Results (microstrain)

Table A1. Quarter–Scale Floor Tests (QSFT) Maximum Tensile Strain Results (microstrain)

Test #		1	2	3	4	5	6	7	8	9	10	11	12	13	14	15	16	17	18	19
Test Series QSFT–_ _C		1A	1B	2A	2B	3A	3B	4A	4B	4C	4D	4E	4F	4G	4H	4I	4J	4K	5A	5B
C4 Explosive Weight		0.6 #	0.6 #	1.24 #	1.24 #	2.48#	2.48#	3.1#	3.1#	3.1#	3.1#	3.1#	3.1#	3.1#	3.1#	3.1#	3.1#	3.1#	4.95#	4.95#
% of full–scale charge		25%	25%	50%	50%	100%	100%	125%	125%	125%	125%	125%	125%	125%	125%	125%	125%	125%	200%	200%
Test date		12/3/92	12/3/92	12/3/92	12/3/92	12/8/92	12/8/92	1/5/93	1/5/93	2/1/93	2/1/93	2/1/93	2/2/93	2/2/93	2/2/93	3/22/93	3/22/93	3/22/93	3/22/93	3/22/93
Gage location	Gage No.													foam	flat gasket	si. rubber	door mat	vinyl	door mat	5 si. pads
center bolt	bolt 1	430	400	800	683	1067	1067	1300	1333	1917	1800	1833	2000	27	27	2233	83	183	167	267
side bolt	bolt 2	323	283	533	467	717	567	833	733	867	593	483	883	143	193	967	260	280	700	433
corner bolt	bolt 3	167	112	133	150	183	227	533	317	367	257	180	367	250	250	533	323	367	967	383
center concrete Z	sg4	35	45	136	120	250	260	380	540	—	2020	2000	2200	110	300	—	50	140	200	500
top rebar X	sg5	45	48	97	79	138	131	245	217	345	379	321	345	26	52	469	41	83	193	169
top rebar Y	sg6	lost	lost	lost	lost	lost	lost	lost	lost	lost	lost	lost	lost	lost	lost	lost	lost	lost	lost	lost
lower rebar Y	sg7	62	67	190	190	414	638	776	569	810	672	603	603	121	162	828	224	86	534	448
lower rebar X	sg8	71	81	255	269	603	734	879	776	1086	966	862	1259	166	241	1207	193	241	655	483
upper concrete X	sg9	38	52	88	80	162	108	220	162	500	360	340	340	70	64	500	74	240	200	220
lower concrete X	sg10	80	90	390	460	1040	1300	1520	1300	1900	1420	1060	1800	186	180	1500	130	170	850	770
anvil X	sg11	120	103	127	113	483	367	200	250	227	190	167	250	100	247	300	283	317	317	467
anvil Y	sg12	117	112	80	73	400	153	167	133	150	127	100	143	115	210	200	133	150	317	483
lower concrete Y	sg13	36	34	70	56	60	24	42	90	130	180	192	550	40	92	1020	70	112	200	200
center stirrup Z	sg14	62	52	131	107	207	203	283	362	—	—	1172	1198	62	134	1759	34	62	138	259

TABLE A2. Quarter-Scale Floor Tests (QFST) Maximum Compressive Strain Results (microstain)

Table A2. Quarter–Scale Floor Tests (QSFT) Maximum Compressive Strain Results (microstrain)

Test #		1	2	3	4	5	6	7	8	9	10	11	12	13	14	15	16	17	18	19
Test Series QSFT–_ _C		1A	1B	2A	2B	3A	3B	4A	4B	4C	4D	4E	4F	4G	4H	4I	4J	4K	5A	5B
C4 Explosive Weight		0.6 #	0.6 #	1.24 #	1.24 #	2.48#	2.48#	3.1#	3.1#	3.1#	3.1#	3.1#	3.1#	3.1#	3.1#	3.1#	3.1#	3.1#	4.95#	4.95#
% of full scale charge		25%	25%	50%	50%	100%	100%	125%	125%	125%	125%	125%	125%	125%	125%	125%	125%	125%	200%	200%
Test date		12/3/92	12/3/92	12/3/92	12/3/92	12/8/92	12/8/92	1/5/93	1/5/93	2/1/93	2/1/93	2/1/93	2/2/93	2/2/93	2/2/93	3/22/93	3/22/93	3/22/93	3/22/93	3/22/93
Gage location	Gage No.													foam	flat gasket	si. rubber	door mat	vinyl	door mat	5 si. pads
center bolt	bolt 1	–100	–100	–167	–117	–217	–333	–233	–167	–400	–233	–167	–333	–183	–290	–267	–300	–333	–767	–800
side bolt	bolt 2	–233	–150	–133	–117	–100	–233	–150	–150	–300	–150	–133	–300	–127	–97	–85	–73	–80	–167	–50
corner bolt	bolt 3	–80	–67	–53	–73	–47	–100	–83	–67	–67	–60	–47	–100	–100	–103	–67	–70	–100	–100	–60
center concrete Z	sg4	–92	–86	–210	–168	–320	–340	–420	–400	—	–760	–700	–640	–290	–340	—	–540	–580	–920	–640
top rebar X	sg5	–41	–31	–28	–20	–14	–45	–10	–90	–69	–52	–52	–52	–66	–84	–97	–95	–134	–207	–138
top rebar Y	sg6	lost	lost	lost	lost	lost	lost	lost	lost	lost	lost	lost	lost	lost	lost	lost	lost	lost	lost	lost
lower rebar Y	sg7	–47	–41	–62	–62	–34	–72	–69	–76	–52	–66	–66	–69	–41	–90	–69	–62	–97	–76	–62
lower rebar X	sg8	–34	–43	–52	–79	–121	–190	–155	–172	–103	–110	–121	–114	–41	241	–52	–86	–62	–138	–103
upper concrete X	sg9	–35	–32	–36	–12	0	–66	–20	–90	0	–160	–140	–150	–64	–72	–160	–100	–100	–280	–100
lower concrete X	sg10	–50	–46	–96	–120	0	–200	–200	–100	0	0	–60	–120	–100	–140	0	–148	–140	–150	–100
anvil X	sg11	–107	–93	–127	–107	–300	–117	–193	–150	–267	–233	–183	–233	–57	–47	–400	–100	–100	–150	–83
anvil Y	sg12	–107	–73	–140	–117	–217	–173	–150	–117	–200	–190	–167	–210	–77	–73	–317	–107	–83	–200	–100
lower concrete Y	sg13	–28	–34	–64	–46	–68	–68	–80	–26	–90	–120	–1140	–60	–28	–56	–140	–74	–72	–150	–60
center stirrup Z	sg14	–103	–98	–217	–186	–328	–338	–379	–345	—	—	–517	–517	–148	–176	–724	–207	–276	–569	–345

Table A3.
Quarter-Scale Floor Tests (QSFT) Maximum Tensile Stress Results (psi)

Table A3. Quarter-Scale Floor Tests (QSFT) Maximum Tensile Stress Results (psi)

Test #		1	2	3	4	5	6	7	8	9	10	11	12	13	14	15	16	17	18	19
Test Series QSFT-__C		1A	1B	2A	2B	3A	3B	4A	4B	4C	4D	4E	4F	4G	4H	4I	4J	4K	5A	5B
C4 Explosive Weight		0.6 #	0.6 #	1.24 #	1.24 #	2.48#	2.48#	3.1#	3.1#	3.1#	3.1#	3.1#	3.1#	3.1#	3.1#	3.1#	3.1#	3.1#	4.95#	4.95#
% of full scale charge		25%	25%	50%	50%	100%	100%	125%	125%	125%	125%	125%	125%	125%	125%	125%	125%	125%	200%	200%
Test date		12/3/92	12/3/92	12/3/92	12/3/92	12/8/92	12/8/92	1/5/93	1/5/93	2/1/93	2/1/93	2/1/93	2/2/93	2/2/93	2/2/93	3/22/93	3/22/93	3/22/93	3/22/93	3/22/93
Gage location	Gage No.													foam	flat gasket	si. rubber	door mat	vinyl	door mat	5 si. pads
center bolt	bolt 1	12,900	12,000	24,000	20,500	32,000	32,000	39,000	40,000	57,500	54,000	55,000	60,000	800	800	67,000	**2,500**	**5,500**	**5,000**	8,000
side bolt	bolt 2	9,700	8,500	16,000	14,000	21,500	17,000	25,000	22,000	26,000	17,800	14,500	26,500	4,300	5,800	29,000	7,800	8,400	21,000	13,000
corner bolt	bolt 3	5,000	3,350	4,000	4,500	5,500	6,800	16,000	9,500	11,000	7,700	5,400	11,000	7,500	7,500	16,000	9,700	11,000	29,000	11,500
center concrete Z	sg4	**175**	225	**680**	**600**	**1,250**	**1,300**	**1,900**	**2,700**	overload	**10,100**	10,000	11,000	550	1,500	overload	250	700	1,000	2,500
top rebar X	sg5	1,300	1,400	**2,800**	**2,300**	**4,000**	3,800	**7,100**	**6,300**	**10,000**	**11,000**	**9,300**	10,000	750	1,500	13,600	1,200	2,400	5,600	4,900
top rebar Y	sg6	lost	lost	lost	lost	lost	lost	lost	lost	lost	lost	lost	lost	lost	lost	lost	lost	lost	lost	lost
lower rebar Y	sg7	**1,800**	**1,950**	**5,500**	**5,500**	**12,000**	**18,500**	22,500	16,500	23,500	19,500	17,500	**17,500**	3,500	4,700	**24,000**	6,500	2,500	15,500	13,000
lower rebar X	sg8	**2,050**	**2,350**	**7,400**	**7,800**	**17,500**	21,300	**25,500**	22,500	**31,500**	28,000	25,000	36,500	4,800	7,000	**35,000**	5,600	7,000	19,000	14,000
upper concrete X	sg9	190	260	440	**400**	**810**	540	**1,100**	810	**2,500**	1,800	1,700	1,700	350	320	**2,500**	370	1,200	1,000	**1,100**
lower concrete X	sg10	400	**450**	**1,950**	**2,300**	**5,200**	**6,500**	**7,600**	**6,500**	**9,500**	**7,100**	**5,300**	**9,000**	930	900	**7,500**	650	850	**4,250**	**3,850**
anvil X	sg11	3,600	**3,100**	3,800	3,400	14,500	11,000	6,000	**7,500**	6,800	5,700	**5,000**	7,500	**3,000**	7,400	9,000	8,500	9,500	9,500	14,000
anvil Y	sg12	**3,500**	**3,350**	**2,400**	**2,200**	12,000	**4,600**	**5,000**	**4,000**	**4,500**	3,800	3,000	**4,300**	3,450	6,300	6,000	4,000	**4,500**	9,500	14,500
lower concrete Y	sg13	180	**170**	**350**	**280**	300	120	**210**	**450**	**650**	**900**	960	**2,750**	200	460	5,100	350	560	1,000	1,000
center stirrup Z	sg14	**1,800**	**1,500**	3,800	3,100	**6,000**	**5,900**	**8,200**	**10,500**	overload	overload	34,000	34,750	1,800	3,900	51,000	1,000	1,800	4,000	7,500

Table A4. Quarter-Scale Floor Tests (QSFT) Maximum Compressive Stress Results (psi)

Table A4. Quarter-Scale Floor Tests (QSFT) Maximum Compressive Stress Results (psi)

Test #		1	2	3	4	5	6	7	8	9	10	11	12	13	14	15	16	17	18	19
Test Series QSFT-__C		1A	1B	2A	2B	3A	3B	4A	4B	4C	4D	4E	4F	4G	4H	4I	4J	4K	5A	5B
C4 Explosive Weight		0.6 #	0.6 #	1.24 #	1.24 #	2.48#	2.48#	3.1#	3.1#	3.1#	3.1#	3.1#	3.1#	3.1#	3.1#	3.1#	3.1#	3.1#	4.95#	4.95#
% of full scale charge		25%	25%	50%	50%	100%	100%	125%	125%	125%	125%	125%	125%	125%	125%	125%	125%	125%	200%	200%
Test date		12/3/92	12/3/92	12/3/92	12/3/92	12/8/92	12/8/92	1/5/93	1/5/93	2/1/93	2/1/93	2/1/93	2/2/93	2/2/93	2/2/93	3/22/93	3/22/93	3/22/93	3/22/93	3/22/93
Gage location	Gage No.													foam	flat gasket	si. rubber	door mat	vinyl	door mat	5 si. pads
center bolt	bolt 1	**-3,000**	**-3,000**	**-5,000**	-3,500	**-6,500**	**-10,000**	**-7,000**	**-5,000**	**-12,000**	**-7,000**	-5,000	**-10,000**	**-5,500**	**-8,700**	**-8,000**	-9,000	-10,000	-23,000	**-24,000**
side bolt	bolt 2	**-7,000**	**-4,500**	**-4,000**	**-3,500**	**-3,000**	**-7,000**	**-4,500**	**-4,500**	**-9,000**	**-4,500**	**-4,000**	**-9,000**	**-3,800**	-2,900	-2,550	-2,200	-2,400	-5,000	-1,500
corner bolt	bolt 3	**-2,400**	-2,000	**-1,600**	-2,200	**-1,400**	**-3,000**	**-2,500**	**-2,000**	**-2,000**	**-1,800**	**-1,400**	**-3,000**	-3,000	-3,100	-2,000	-2,100	-3,000	**-3,000**	-1,800
center concrete Z	sg4	-460	-430	-1,050	-840	-1,600	-1,700	**-2,100**	**-2,000**	overload	-3,800	-3,500	-3,200	**-1,450**	-1,700	overload	**-2,700**	-2,900	**-4,600**	-3,200
top rebar X	sg5	-1,200	-900	-800	-580	-400	-1,300	**-300**	**-2,600**	-2,000	-1,500	-1,500	-1,500	-1,900	**-2,450**	-2,800	**-2,750**	-3,900	-6,000	-4,000
top rebar Y	sg6	lost	lost	lost	lost	lost	lost	lost	lost	lost	lost	lost	lost	lost	lost	lost	lost	lost	lost	lost
lower rebar Y	sg7	-1,350	-1,200	-1,800	-1,800	-1,000	-2,100	-2,000	-2,200	-1,500	-1,900	-1,900	-2,000	-1,200	**-2,600**	-2,000	**-1,800**	-2,800	-2,200	-1,800
lower rebar X	sg8	-1,000	-1,250	-1,500	-2,300	-3,500	**-5,500**	**-4,500**	-5,000	-3,000	-3,200	-3,500	-3,300	-1,200	7,000	-1,500	-2,500	-1,800	-4,000	-3,000
upper concrete X	sg9	-175	-160	-180	-60	0	**-330**	**-100**	**-450**	0	**-800**	**-700**	**-750**	-320	-360	-800	**-500**	-500	-1,400	-500
lower concrete X	sg10	-250	-230	-480	-600	0	**-1,000**	**-1,000**	-500	0	0	-300	-600	-500	-700	0	**-740**	-700	-750	-500
anvil X	sg11	-3,200	-2,800	-3,800	-3,200	-9,000	-3,500	-5,800	-4,500	-8,000	-7,000	-5,500	-7,000	-1,700	**-1,400**	**-12,000**	-3,000	-3,000	-4,500	-2,500
anvil Y	sg12	-3,200	-2,200	-4,200	-3,500	-6,500	-5,200	-4,500	-3,500	-6,000	-5,700	-5,000	-6,300	-2,300	-2,200	-9,500	-3,200	-2,500	-6,000	-3,000
lower concrete Y	sg13	-140	-170	-320	-230	**-340**	-340	**-400**	**-130**	-450	-600	-5,700	-300	**-140**	**-280**	-700	**-370**	-360	-750	-300
center stirrup Z	sg14	-3,000	-2,850	-6,300	-5,400	-9,500	**-9,800**	**-11,000**	**-10,000**	overload	overload	**-15,000**	-15,000	-4,300	-5,100	-21,000	-6,000	-8,000	-16,500	-10,000

Bold indicates permanent offset for this measurement direction

Table A5. Quarter-Scale Floor Tests (QSFT) Maximum Tensile Strain Safety Factors for Yielding

Table A5. Quarter-Scale Floor Tests (QSFT) Maximum Tensile Strain Safety Factors for Yielding

Test #		1	2	3	4	5	6	7	8	9	10	11	12	13	14	15	16	17	18	19
Test Series QSFT-__C		1A	1B	2A	2B	3A	3B	4A	4B	4C	4D	4E	4F	4G	4H	4I	4J	4K	5A	5B
C4 Explosive Weight		0.6 #	0.6 #	1.24 #	1.24 #	2.48#	2.48#	3.1#	3.1#	3.1#	3.1#	3.1#	3.1#	3.1#	3.1#	3.1#	3.1#	3.1#	4.95#	4.95#
% of full scale charge		25%	25%	50%	50%	100%	100%	125%	125%	125%	125%	125%	125%	125%	125%	125%	125%	125%	200%	200%
Test date		12/3/92	12/3/92	12/3/92	12/3/92	12/8/92	12/8/92	1/5/93	1/5/93	2/1/93	2/1/93	2/1/93	2/2/93	2/2/93	2/2/93	3/22/93	3/22/93	3/22/93	3/22/93	3/22/93
Gage location	Gage No.													foam	flat gasket	si. rubber	door mat	vinyl	door mat	5 si. pads
center bolt	bolt 1	4.7	5.0	2.5	2.9	1.9	1.9	1.5	1.5	1.0	1.1	1.1	1.0	75.0	75.0	**0.9**	24.0	10.9	12.0	7.5
side bolt	bolt 2	6.2	7.1	3.7	4.3	2.8	3.5	2.4	2.7	2.3	3.4	4.1	2.3	14.0	10.3	2.1	7.7	7.1	2.9	4.6
corner bolt	bolt 3	12.0	17.9	15.0	13.3	10.9	8.8	3.7	6.3	5.5	7.8	11.1	5.5	8.0	8.0	3.7	6.2	5.5	2.1	5.2
center concrete Z	sg4	3.5	2.8	**0.9**	**1.0**	**0.5**	**0.5**	**0.3**	**0.2**	—	**0.1**	**0.1**	**0.1**	1.1	**0.4**	—	2.5	**0.9**	**0.6**	**0.2**
top rebar X	sg5	44.6	41.4	20.7	25.2	14.5	15.3	8.2	9.2	5.8	5.3	6.2	5.8	77.3	38.7	4.3	48.3	24.2	10.4	11.8
top rebar Y	sg6	lost	lost	lost	lost	lost	lost	lost	lost	lost	lost	lost	lost	lost	lost	lost	lost	lost	lost	lost
lower rebar Y	sg7	32.2	29.7	10.5	10.5	4.8	3.1	2.6	3.5	2.5	3.0	3.3	3.3	16.6	12.3	2.4	8.9	23.2	3.7	4.5
lower rebar X	sg8	28.3	24.7	7.8	7.4	3.3	2.7	2.3	2.6	1.8	2.1	2.3	1.6	12.1	8.3	1.7	10.4	8.3	3.1	4.1
upper concrete X	sg9	3.3	2.4	1.4	1.6	**0.8**	1.1	**0.6**	**0.8**	**0.2**	**0.3**	**0.4**	**0.4**	1.8	1.9	**0.2**	1.7	**0.5**	**0.6**	**0.6**
lower concrete X	sg10	1.6	1.4	**0.3**	**0.3**	**0.1**	**0.1**	**0.1**	**0.1**	**0.1**	**0.1**	**0.1**	**0.1**	**0.7**	**0.7**	**0.1**	1.0	**0.7**	**0.1**	**0.2**
anvil X	sg11	10.0	11.6	9.5	10.6	2.5	3.3	6.0	4.8	5.3	6.3	7.2	4.8	12.0	4.9	4.0	4.2	3.8	3.8	2.6
anvil Y	sg12	10.3	10.7	15.0	16.4	3.0	7.8	7.2	9.0	8.0	9.5	12.0	8.4	10.4	5.7	6.0	9.0	8.0	3.8	2.5
lower concrete Y	sg13	3.4	3.6	1.8	2.2	2.1	5.2	3.0	1.4	1.0	**0.7**	**0.6**	**0.2**	3.1	1.3	**0.1**	1.8	1.1	**0.6**	**0.6**
center stirrup Z	sg14	32.2	38.7	15.3	18.7	9.7	9.8	7.1	5.5	—	—	1.7	1.7	32.2	14.9	1.1	58.0	32.2	14.5	7.7

Table A6. Quarter-Scale Floor Tests (QFST) Maximum Compressive Strain Safety Factor

Table A6. Quarter-Scale Floor Tests (QSFT) Maximum Compressive Strain Safety Factors for Yielding

Test #		1	2	3	4	5	6	7	8	9	10	11	12	13	14	15	16	17	18	19
Test Series QSFT-__C		1A	1B	2A	2B	3A	3B	4A	4B	4C	4D	4E	4F	4G	4H	4I	4J	4K	5A	5B
C4 Explosive Weight		0.6 #	0.6 #	1.24 #	1.24 #	2.48#	2.48#	3.1#	3.1#	3.1#	3.1#	3.1#	3.1#	3.1#	3.1#	3.1#	3.1#	3.1#	4.95#	4.95#
% of full scale charge		25%	25%	50%	50%	100%	100%	125%	125%	125%	125%	125%	125%	125%	125%	125%	125%	125%	200%	200%
Test date		12/3/92	12/3/92	12/3/92	12/3/92	12/8/92	12/8/92	1/5/93	1/5/93	2/1/93	2/1/93	2/1/93	2/2/93	2/2/93	2/2/93	3/22/93	3/22/93	3/22/93	3/22/93	3/22/93
Gage location	Gage No.													foam	flat gasket	si. rubber	door mat	vinyl	door mat	5 si. pads
center bolt	bolt 1	20.0	20.0	12.0	17.1	9.2	6.0	8.6	12.0	5.0	8.6	12.0	6.0	10.9	6.9	7.5	6.7	6.0	2.6	2.5
side bolt	bolt 2	8.6	13.3	15.0	17.1	20.0	8.6	13.3	13.3	6.7	13.3	15.0	6.7	15.8	20.7	23.5	27.3	25.0	12.0	40.0
corner bolt	bolt 3	25.0	30.0	37.5	27.3	42.9	20.0	24.0	30.0	30.0	33.3	42.9	20.0	20.0	19.4	30.0	28.6	20.0	20.0	33.3
center concrete Z	sg4	13.0	14.0	5.7	7.1	3.8	3.5	2.9	3.0	—	1.6	1.7	1.9	4.1	3.5	—	2.2	2.1	1.3	1.9
top rebar X	sg5	48.3	64.4	72.5	100.0	145.0	44.6	193.3	22.3	29.0	38.7	38.7	38.7	30.5	23.7	20.7	21.1	14.9	9.7	14.5
top rebar Y	sg6	lost	lost	lost	lost	lost	lost	lost	lost	lost	lost	lost	lost	lost	lost	lost	lost	lost	lost	lost
lower rebar Y	sg7	43.0	48.3	32.2	32.2	58.0	27.6	29.0	26.4	38.7	30.5	30.5	29.0	48.3	22.3	29.0	32.2	20.7	26.4	32.2
lower rebar X	sg8	58.0	46.4	38.7	25.2	16.6	10.5	12.9	11.6	19.3	18.1	16.6	17.6	48.3	-8.3	38.7	23.2	32.2	14.5	19.3
upper concrete X	sg9	34.3	37.5	33.3	100.0	#DIV/0!	18.2	60.0	13.3	#DIV/0!	7.5	8.6	8.0	18.8	16.7	7.5	12.0	12.0	4.3	12.0
lower concrete X	sg10	24.0	26.1	12.5	10.0	#DIV/0!	6.0	6.0	12.0	#DIV/0!	#DIV/0!	20.0	10.0	12.0	8.6	#DIV/0!	8.1	8.6	8.0	12.0
anvil X	sg11	11.2	12.9	9.5	11.2	4.0	10.3	6.2	8.0	4.5	5.1	6.5	5.1	21.2	25.7	3.0	12.0	12.0	8.0	14.4
anvil Y	sg12	11.2	16.4	8.6	10.3	5.5	6.9	8.0	10.3	6.0	6.3	7.2	5.7	15.7	16.4	3.8	11.2	14.4	6.0	12.0
lower concrete Y	sg13	42.9	35.3	18.8	26.1	17.6	17.6	15.0	46.2	13.3	10.0	1.1	20.0	42.9	21.4	8.6	16.2	16.7	8.0	20.0
center stirrup Z	sg14	19.3	20.4	9.2	10.7	6.1	5.9	5.3	5.8	—	—	3.9	3.9	13.5	11.4	2.8	9.7	7.2	3.5	5.8

#DIV/0! indicates computationally equal to infinity

Bold indicates yielding (SF<1)

Appendix B

Fabrication and Instrumentation Drawing

FIGURE 20